

# **SANDIA REPORT**

SAND2001-1783

Unlimited Distribution

Printed January 2002

## **Statistical Validation of Engineering and Scientific Models: A Maximum Likelihood Based Metric**

Richard G. Hills and Timothy G. Trucano

Prepared by

Sandia National Laboratories

Albuquerque, New Mexico 87185 and Livermore, California 94550

Sandia is a multiprogram laboratory operated by Sandia Corporation,  
a Lockheed Martin Company, for the United States Department of  
Energy under Contract DE-AC04-94AL85000

Approved for public release; further dissemination unlimited.



**Sandia National Laboratories**

Issued by Sandia National Laboratories, operated for the United States Department of Energy by Sandia Corporation.

**NOTICE:** This report was prepared as an account of work sponsored by an agency of the United States Government. Neither the United States Government nor any agency thereof, nor any of their employees, nor any of their contractors, subcontractors, or their employees, makes any warranty, express or implied, or assumes any legal liability or responsibility for the accuracy, completeness, or usefulness of any information, apparatus, product, or process disclosed, or represents that its use would not infringe privately owned rights. Reference herein to any specific commercial product, process, or service by trade name, trademark, manufacturer, or otherwise, does not necessarily constitute or imply its endorsement, recommendation, or favoring by the United States Government, any agency thereof or any of their contractors or subcontractors. The views and opinions expressed herein do not necessarily state or reflect those of the United States Government, any agency thereof or any of their contractors.

Printed in the United States of America. This report has been reproduced directly from the best available copy.

Available to DOE and DOE contractors from

U.S. Department of Energy  
Office of Scientific and Technical Information  
P.O. Box 62  
Oak Ridge, TN 37831

Telephone: (865)576-8401  
Facsimile: (865)576-5782  
E-Mail: [reports@adonis.osti.gov](mailto:reports@adonis.osti.gov)  
Online ordering: <http://www.doe.gov/bridge>

Available to the public from

U.S. Department of Commerce  
National Technical Information Service  
5285 Port Royal Rd  
Springfield, VA 22161

Telephone: (800)553-6847  
Facsimile: (703)605-6900  
E-Mail: [orders@ntis.fedworld.gov](mailto:orders@ntis.fedworld.gov)  
Online order: <http://www.ntis.gov/ordering.htm>



SAND2001-1783  
Unlimited Release  
Printed January 2002

# **Statistical Validation of Engineering and Scientific Models: A Maximum Likelihood Based Metric**

Richard G. Hills  
Department of Mechanical Engineering  
New Mexico State University  
Las Cruces, New Mexico 88003

Timothy G. Trucano  
Optimization and Uncertainty Estimation  
Sandia National Laboratories  
P. O. Box 5800  
Albuquerque, New Mexico 87185-0819

## **Abstract**

Two major issues associated with model validation are addressed here. First, we present a maximum likelihood approach to define and evaluate a model validation metric. The advantage of this approach is it is more easily applied to nonlinear problems than the methods presented earlier by Hills and Trucano (1999, 2001); the method is based on optimization for which software packages are readily available; and the method can more easily be extended to handle measurement uncertainty and prediction uncertainty with different probability structures. Several examples are presented utilizing this metric. We show conditions under which this approach reduces to the approach developed previously by Hills and Trucano (2001).

Secondly, we expand our earlier discussions (Hills and Trucano, 1999, 2001) on the impact of multivariate correlation and the effect of this on model validation metrics. We show that ignoring correlation in multivariate data can lead to misleading results, such as rejecting a good model when sufficient evidence to do so is not available.

(Page left blank)

## Acknowledgements

This report is an account of contract research (Doc. # AX-0620) performed by the first author in cooperation with the second author during the 2000 Fiscal Year. We thank Robert G. Easterling for reviewing this work.

(Page left blank)

# Contents

Abstract .....	3
Contents.....	7
List of Figures .....	9
List of Tables.....	11
1.0 Introduction .....	13
1.1 Introduction.....	13
1.2 What are we actually testing? .....	13
1.3 What do these metrics provide?.....	14
1.4 Our Focus.....	15
2.0 Overview of Previous Years' Work .....	17
2.1 Introduction.....	17
2.2 Year 1 .....	17
2.3 Year 2.....	18
2.4 Year 3.....	19
3.0 The Test Cases .....	21
3.1 Introduction.....	21
3.2 The Heat Conduction Experiment .....	21
3.2.1 The Experiment .....	21
3.2.2 The Measurements.....	22
3.2.3 The Numerical Model.....	23
3.2.4 Probability Models for Measurements and Model Parameters.....	25
3.3 Impact of Aluminum on Aluminum .....	26
3.3.1 Experimental Data .....	27
3.3.2 The Measurement Data.....	28
3.3.3 The Model Parameters.....	31
3.3.4 The Physical Model .....	33
4.0 Maximum Likelihood Method .....	37
4.1 Introduction.....	37
4.2 Geometry.....	39
4.3 Maximum Likelihood Procedure .....	42
4.4 Significance of the Estimated Parameters.....	43
4.5 Discussion.....	45
5.0 Applications .....	49
5.1 Introduction.....	49
5.2 Application to the Heat Conduction Data .....	49
5.3 Application to Shock Physics Application.....	51
5.4 Non-Normally Distributed Parameters and Measurements .....	52
6.0 Equivalence to Previous Metric .....	57
7.0 Univariate Confidence Intervals.....	61
7.1 Introduction.....	61

7.2 Two Measurement Times .....	63
7.3 More than 2 Measurement Times .....	66
7.4 Correlation and the Maximum Likelihood Method .....	69
8.0 Discussion and Recommendations .....	71
8.1 The Approach.....	71
8.2 Accomplishments Over the Past Three Years.....	71
8.3 Recommendations.....	72
References .....	75

## List of Figures

Figure 3.1:	Heat Conduction Apparatus and Computational Domain .....	22
Figure 3.2:	Temperature as a Function of Time .....	25
Figure 3.3:	The Symmetric Impact of Two Aluminum Plates. ....	26
Figure 3.4:	Explosive-Metal Geometry Feasible for Performing Shock Hugoniot Measurements. ....	27
Figure 3.5:	Predicted and Observed Shock Speeds as a Function of Particle Speed: The predicted speeds are based on tri-linear interpolation using the values of Table 3.7.....	35
Figure 4.2:	Maximum Likelihood Estimate .....	43
Figure 7.1:	Experimental and Predicted Data. Time zero data are not shown. Confidence intervals are based on normal distributions at 95% confidence and univariate statistics. ....	61
Figure 7.2:	Experimental and Predicted Data. Time zero data are not shown. Combined confidence intervals are based on normal distributions at 95% confidence and univariate statistics.....	62
Figure 7.3:	95% Confidence Intervals on the Differences – 2 Measurements: Solid ellipse includes correlation, dashed ellipse ignores correlation, rectangle represents univariate confidence intervals, point is the difference. ....	66
Figure 7.4:	95% Confidence Intervals on the Differences – 10 measurements: Solid ellipse includes correlation, dashed ellipse ignores correlation, rectangle represents univariate confidence intervals, point is the difference. ....	68

(Page left blank)

## List of Tables

Table 3.1:	Thermocouple Axial Locations.....	23
Table 3.2:	Temperatures and Sensitivity Coefficients .....	23
Table 3.3:	Model Parameters Statistics.....	24
Table 3.4:	Predicted and Observed Shock Speeds (m/s).....	29
Table 3.5:	Calibration Constants.....	31
Table 3.6:	Distribution Parameters for Alternate Probability Models .....	33
Table 3.7:	Interpolation Table of Shock Speed as a Function of Particle Speed and Model Parameters .....	34
Table 5.1:	The Most Likely Model Parameters for the Heat Conduction Data .....	50
Table 5.2:	Statistics for the Shock Physics Application.....	51
Table 5.3:	The Most Likely Model Parameters for the Shock Physics Application ...	52
Table 5.4:	Distribution Parameters for Alternate Probability Models .....	53
Table 5.5:	Maximum Likelihood Parameters.....	55

(Page left blank)

## **1.0 Introduction**

### **1.1 Introduction**

This report is a third in a series of reports describing issues related to model validation. The focus of the past two years work has been on the development of statistical based model validation metrics that use differences between model predictions and experimental measurements. The measurements can be multiple measurements from a single experiment or single measurements from multiple experiments, or a combination of these. The primary contrast to the work by other authors is we explicitly account for correlation between the differences induced by model structure. Correlation in these differences will be significant for models that provide predictions of multiple quantities, such as pressure or stress as a function of time or space. If a field-equation based model over predicts a temperature or pressure at some location or time, it also tends to over predict the temperature or pressure at an adjacent location or time. This is the nature of the models that we are most concerned with and this structure must be properly accounted for if one is to appropriately apply statistical methods.

The application of statistical methods requires some prior knowledge of the underlying form for the uncertainty of the random variables. Our assumption here is such knowledge is available for the measurements and for the uncertain parameters that make up the model. Other approaches exist (such as possibility theory; see Dubois and Prade, 1988) that allow one to relax the required knowledge of uncertainty. But relaxing these assumptions comes with a cost. The less one knows about a system, the less precise one can be about the behavior of a particular realization of the system. The methods presented here represent a near-upper bound of the knowledge required to define uncertainty. On the other hand, these methods also represent a near upper bound on the precision to which one can resolve model validity. Generally, other methods may be less sensitive to the lack of knowledge of the underlying uncertainties, but they will also be less sensitive to bad predictive models. If the planned application of the model is critical, and if the corresponding engineering design is not sufficiently conservative, then the acceptance of a bad model can lead to undesirable results. On the other hand, if a less sensitive approach (such as possibility theory) is used with the model to design the application with sufficient conservatism, then the constraints required by the statistical approaches to characterize the uncertainty for model validation may not be required.

### **1.2 What are we actually testing?**

Given a set of measurements and a set of model predictions, we develop a statistical based metric to measure the inconsistency between the two. Specifically, we look for statistically significant evidence that the model predictions are not consistent with the

experimental observations. These metrics can be used in one of two ways. The first is to evaluate the probability that a valid model would give the observed differences between the model predictions and experimental observations. Such probabilities can be used with similar probabilities from other independent validation tests to evaluate the joint probability for a suite of validation tests. We can also use these metrics to define pass-fail criteria – say at the 95% confidence level – that there is sufficient evidence to reject the model.

The statistical test performed here is based on controlling the probability of a Type I error (Brownlee, 1965). In the context of our model validation methodology, a Type I error is committed when we reject a good model. To reduce the chances of doing this to an acceptable level, we give the benefit of doubt to the model. For example, if we test at the 95% confidence level, we define the acceptance/rejection boundary of our metric such that if the model were valid (and our models for the corresponding uncertainties), then we would reject a good model only 5% of the time. We have 95% confidence that we did not reject a good model. We do not have 95% confidence that we have accepted a good model.

In contrast, a Type II error (Brownlee, 1965) is committed, in the present context, when we fail to reject a bad model. Ideally, we would like a test that has a small probability of rejecting a good model with a large probability of rejecting a bad model. Unfortunately, these goals are somewhat contradictory. We can measure this effect by looking at the power of the test, given an alternative hypothesis or model. The power of a test is the probability of correctly rejecting the null hypothesis or bad model (Brownlee, 1965). Ideally, we would like a test that is as powerful as possible, say 95%, while maintaining 95% confidence that we did not reject a good model. Unfortunately, the time and money required to execute a test that has 95% confidence and a power of 95% may likely exceed available resources. This requires much high quality data. Because of this, we typically define the test at a certain confidence level so that we aren't likely to reject a good model and accept that we may fail to reject a bad model.

Engineering and scientific judgment and consensus building are required to develop a suite of validation tests such that if a model is not rejected, the consensus is that the model is valid for the intended application. Limiting our focus to questions of validity for a particular application is a much more feasible undertaking since we can restrict the range of conditions for which such a model is to be applied. However, even with this restriction, scientific/engineering judgment is required to develop the suite of appropriate validation experiments. This is because our validation experiments will generally not exactly reflect the anticipated application of our model.

### ***1.3 What do these metrics provide?***

What do statistical validation metrics provide that simple graphical or tabular

comparisons of experimental results to model predictions do not? Statistical validation metrics provide probabilistic measures of consistency between model predictions and experimental observations, given that the model is correct. This requires that the uncertainty in the validation exercise be quantified. The application of statistical methods to model validation is very useful to the decision maker in that they also provide quantification of the ability of the experiment to resolve differences between model predictions and experimental observations. If the uncertainty in the validation exercise is large (due to few or inaccurate data, or highly uncertain model parameters or boundary conditions) compared to the acceptable uncertainty for an application, then the model validation experiments may not be able to adequately resolve the validity of the model for that application. This reemphasizes the point made earlier. The testing performed here evaluates the consistency of the model predictions with the experimental measurements, relative to the uncertainty (actually the modeled uncertainty) in the validation exercise. This provides important quantitative information to scientists/engineers that will help to develop a consensus on whether there is a sufficient body of data showing adequate consistency between model predictions and experimental observations for a particular application.

#### **1.4 Our Focus**

Here we develop statistically rigorous metrics to test for consistency between prediction and experiment. This is not as easy of a task as it first appears due to the form of our models. Our models are typically based on field equations (conservation equations) and are multivariate in nature. Our models predict behavior of the state variables over time, space, or both. These models contain parameters that are used to characterize material properties, geometry, and boundary and initial conditions. The values of these parameters are measured or controlled through the design of the experiment and will contain uncertainty. Since the model predictions are dependent on the values of these parameters, the model predictions will also be uncertain. In addition, the uncertainty in the model predictions will also be correlated due to uncertainty in the model parameters. If the value for a certain model parameter is larger than the true value, then it will generally effect not only the model prediction at some location and time, but will affect the model prediction at adjacent locations and times. For example, if a predicted temperature in a heat-conducting solid is high, there is an increased likelihood that the predicted temperature at an adjacent location in space or time will be high. The errors in these two predicted temperatures are systematic and will be correlated over multiple realizations of the experiments due to the model's dependence of the model parameters.

If our model testing metrics are based on point wise differences between the predictions and the experimental observations, then these differences will likewise be correlated simply because the model predictions are correlated. This is true even if the measurements are not. The difficulty introduced by this correlation is that its effect must be accounted for if the metric is to be statistically correct. The structure of the correlation

in the predictions will be directly related to the structure of the model. The complex structure of this correlation is one of the primary reasons why one has not historically seen statistical techniques applied to model validation for the complex predictive models that we are concerned with. The assumption that the differences between the predictions and the experimental observations are independent for different times and locations is generally not valid. Techniques that are based on this assumption will therefore give misleading results.

Fortunately, the increased power of today's computers allows us to use the model itself to account for this correlation. The focus of the present work is to emphasize that such techniques are now entering the main stream, and to use these techniques as tools to develop statistically based metrics to test for model validity. We emphasize that we are not developing anything new from a statistical perspective, we are simply using existing tools to extend the applications of statistical techniques to increasingly complex computational problems. We will illustrate these extensions through the use of several example problems in later chapters.

## **2.0 Overview of Previous Years' Work**

### **2.1 Introduction**

This report represents the third in a series on statistical model validation metrics. Here we provide an overview of the work presented in the previous two reports and an overview of the work to be presented here.

### **2.2 Year 1**

The primary focus of the first year report (Hills and Trucano, 1999) was to provide background on model validation using statistical methods and to provide a survey of the associated literature. The report was written at the level of the reader who has at least a rudimentary understanding of statistical concepts. The overview addressed the propagation of model parameter uncertainty through a model to estimate the uncertainty in the model predictions due to parameter uncertainty. The literature is very rich on this subject and only a brief review was provided. The year 1 discussion illustrated three approaches to the propagation of uncertainty; 1) direct evaluation for linear models; 2) sensitivity analysis and 3) Monte Carlo analysis. The tutorial illustrated the effects of correlation between model parameters and correlation between model predictions.

Four physical applications were considered: a simple linear model, a model for a damped spring-mass system, a transient thermal conduction model, and a nonlinear transient convective-diffusive model based on Burger's equation. The last three examples were nonlinear in the model parameters. The results showed that for several of the cases considered, including several of the nonlinear cases, the sensitivity analysis can provide comparable results to the Monte Carlo approach for estimates of the expected value and standard deviation of the model predictions. However, this was not the case for the highly nonlinear spring-mass system near resonance.

Several forms of model validation methodology using statistical methods were discussed. One methodology, which we term scientific validation, asked the following question: Is the difference between model predictions and experimental observations significant relative to the uncertainty in the validation exercise? The second form, which we term engineering validation, asked the following question: Is the difference between model predictions and experimental observations significant relative to the uncertainty in the validation exercise, plus an acceptable error?

Both forms of model validation require statistical models for the uncertainty in the differences between the model predictions and the experimental measurements. One approach to develop a statistical model is to use these differences directly. The literature

is rich on this approach to statistical characterization. Unfortunately, an adequate quantity of such data is generally not available for the validation of complex engineering models. Compounding this problem is that for models we are typically interested in, there will almost always be correlation in the differences between model predictions and experiments at adjacent measurement locations and times. The result is that the simplest assumption of uncorrelated differences, at different times and locations, is not valid. The form of this correlation is usually as complex as the model, and the assumptions used by standard techniques (such as time series techniques) to estimate this correlation from the set of differences are generally not appropriate.

A different approach to estimate the correlation structure in the differences between model prediction and experimental observations is to use the predictive model itself. This approach shifts the work from characterizing the uncertainty in the differences to characterizing the uncertainty in the model parameters and in the experimental measurements. This second approach is appropriate when it is easier to generate sufficient data to characterize model parameters (such as thermal conductivity) than it is to repeat the validation experiments many independent times. This approach utilizes techniques developed for uncertainty quantification (such as sensitivity analysis and Monte Carlo analysis) to propagate the model parameter uncertainty through the model to develop a model for prediction uncertainty. This prediction uncertainty is then used, together with a model for measurement uncertainty, to develop an uncertainty model for the differences between the predictions and the experimental observations. The advantage of this approach is if there is an adequate model for the measurement uncertainty (obtained from previous experience with similar measurement devices or experiments) and an understanding of the uncertainty in the model parameters going into the model, then adequate information is present to characterize the uncertainty in the differences – *without repeated realizations of the validation experiment*. A down side (or perhaps an upside) is one must fully understand the sources of model and experimental uncertainty to include them in the analysis. If significant sources of uncertainty are neglected, then the model is more likely to fail the validation test.

The damped spring-mass system application was used to show how such a propagation of uncertainty could be used to develop a statistical metric to test for model validity. This metric was demonstrated for a spring mass system using two measurements taken from simulated validation experiments. Both Monte Carlo and sensitivity analysis methods were applied to this system near resonance.

### **2.3 Year 2**

The second year work of this project (Hills and Trucano, 2001) extended the concepts presented during first year to a shock physics application of interest to Sandia National Laboratories. Both of the approaches discussed above to characterize the uncertainty in the differences between predictions and observations were illustrated in the report of the

second year work. In the first approach, the model for the uncertainty was estimated from the differences directly. This approach could be used because 1) a sufficient quantity of data was available from shock physics experiments, and 2) a linear trend in the data could be easily removed to allow for the characterization of the uncertainty in these differences. In the second approach, we characterized the uncertainty in the model parameters and propagated this uncertainty through the model to develop a model for prediction uncertainty. The model was combined with a model for measurement uncertainty to obtain a model for the uncertainty in the differences between the predictions and the experimental observations. Finally, we presented a variation of the second approach where the validation metric was modified to reflect the desired application of the model. This approach recognizes that the model validation experiments are not necessarily exact or even near replicates of the desired application of the model. As such, a model of the application was used to modify the validation metric so that the validation data was weighted in a fashion appropriate for the application.

The above three approaches were demonstrated using data and a numerical model from shock wave physics. We applied the Eulerian shock wave physics computer code CTH (McGlaun, *et al.*, 1990; Bell *et al.*, 1998; Hertel and Kerley, 1998) to model the impact of an aluminum plate with an equal sized, but initially stationary, aluminum plate at velocities in the kilometer per second regime. Model predictions for shock wave speed were tested against experimental measurements using the three statistical based approaches discussed above. The probability of consistency was evaluated and also used to test consistency at 95% confidence level for each example.

### **2.4 Year 3**

In the present work, we focus on the development of a metric based on maximum likelihood. This approach, as implemented here, does not require that we fully characterize the uncertainty in the model predictions, but rather that we search through the model prediction space (using commonly available optimization algorithms) to find likely values for the model parameters, given their uncertainty and the uncertainty in the experimental measurements. We then look at the probability of obtaining such parameters if the model were correct. While this approach at first seems different from those developed previously, it results in the same metric for models that are locally linear in the model parameters with model parameters and experimental measurements that are normally (or multi normally) distributed. We show this equivalence in Chapter 6.

In addition to the development of the maximum likelihood based metric, we provide some additional background on the effect of correlation in model-experiment differences. Specifically, we address the importance of accounting for correlation in model testing metrics, and show how ignoring such correlation can increase our chances of accepting a bad model, or increase our chances of rejecting a good model, depending on the form of the correlation.

(Page left blank)

## **3.0 The Test Cases**

### **3.1 Introduction**

Two test cases are presented to demonstrate the model validation methodology developed here. The first is an experiment that was designed specifically for model validation (Voth and Gill, 1999). This case is for a carefully controlled, transient, heat conduction experiment designed to test models for thermal contact resistance. Here we use temperature measurements taken from thermal couple time traces to illustrate how data from a few measurement locations can be used to test a model. The intent of this test case is to show how such metrics can be applied when we have very little experimental data. The prediction differences from this data are highly correlated, necessitating the use of multivariate metrics that account such correlation.

The second test case is the one-dimensional impact of an aluminum plate on an aluminum plate considered previously (Hills and Trucano, 2001). Rather than using a sensitivity analysis, as we reported previously, we apply a response surface approach here. This approach can be more easily generalized to highly nonlinear problems. We choose to use this test problem so that the results of previous work (Hills and Trucano, 2001) can be compared to the results of the methodology developed here.

### **3.2 The Heat Conduction Experiment**

In an effort to study and test models for thermal contact resistance, an experimental program was supported through the ASCI Sub-Grid Physics Area and MAVEN. Here we provide a brief overview of the experiment and the model. A more detailed description is provided in Voth and Gill (1999).

#### **3.2.1 The Experiment**

The experimental apparatus is illustrated in Figure 3.1. Two coaxial hollow right circular cylinders are pressed together with a known load to study models for contact resistance. Hollow cylinders were used to minimize variations in shear stress across the contact interface. The entire assembly was enclosed in an evacuated bell jar to minimize heat transfer to the environment and to remove trapped air from the contact interface. Each of the 304 stainless steel cylinders were instrumented with several vertical columns of 7 T-type thermocouples located on the surface of the cylinders. The axial locations of these thermocouples are listed in Table 3.1. The top cylinder was heated from above and the bottom cylinder cooled from below. Temperature responses were recorded at one-second intervals during the transient phase and at 60-second intervals during the near steady-state phase of the experiment.

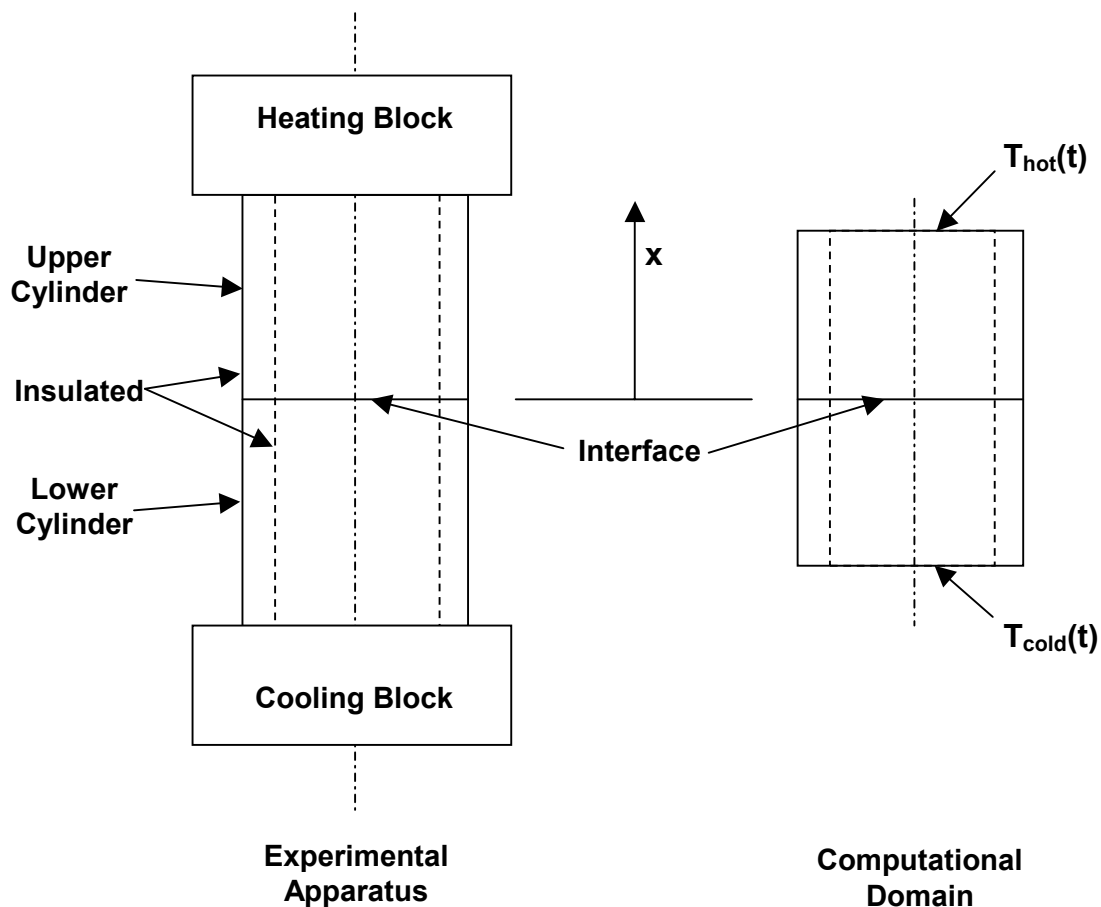


**Figure 3.1: Heat Conduction Apparatus and Computational Domain**

### 3.2.2 The Measurements

We use only a very small subset of the available temperature measurements to illustrate the use of validation metrics when experimental data are limited. This data was sampled from the time trace of data taken from the two thermal couples at station TC7 as listed in Table 3.1. The data was sampled at only 10 times. These times are shown in Table 3.2. The readings from the two thermal couples were averaged, resulting in the average measurements (denoted as measurements) tabulated in Table 3.2. Also shown are estimates of the standard deviation for the average measurements as provided by Dowding (2000). These were obtained by using temperatures at similar stations, for each time. The other items in Table 3.2 will be discussed below.

**Table 3.1: Thermocouple Axial Locations**

Thermocouple	Axial Location (mm)
TC1	61.7
TC2	52.2
TC3	42.7
TC4	33.1
TC5	23.6
TC6	14.1
TC7	4.5
TC8	-4.6
TC9	-14.1
TC10	-23.6
TC11	-33.1
TC12	-42.7
TC13	-52.2
TC14	-61.7

**Table 3.2: Temperatures and Sensitivity Coefficients**

Time s	Measurement °C	$\sigma$ °C	Prediction °C	$\partial T/\partial \alpha_1$ °C	$\partial T/\partial \alpha_2$ °C	$\partial T/\partial \alpha_3$ °C
1.73	29.96	0.1536	29.80	$6.494 \times 10^{-8}$	$-2.483 \times 10^{-13}$	$-4.973 \times 10^{-12}$
570.7	44.94	0.3565	45.09	$6.176 \times 10^{-1}$	$-2.048 \times 10^{-6}$	$-9.633 \times 10^{-4}$
1140.6	53.97	0.3363	54.44	$4.352 \times 10^{-1}$	$-1.281 \times 10^{-6}$	$-1.155 \times 10^{-3}$
1710.5	58.23	0.3216	58.87	$2.837 \times 10^{-1}$	$-6.762 \times 10^{-7}$	$-1.217 \times 10^{-3}$
2341.4	60.55	0.3092	61.28	$1.911 \times 10^{-1}$	$-3.081 \times 10^{-7}$	$-1.251 \times 10^{-3}$
2941.3	61.31	0.3124	62.07	$1.420 \times 10^{-1}$	$-1.186 \times 10^{-7}$	$-1.252 \times 10^{-3}$
3541.2	61.56	0.3121	62.35	$1.225 \times 10^{-1}$	$-4.366 \times 10^{-8}$	$-1.252 \times 10^{-3}$
4141.1	61.67	0.3172	62.45	$1.153 \times 10^{-1}$	$-1.577 \times 10^{-8}$	$-1.253 \times 10^{-3}$
4741.0	61.72	0.3189	62.50	$1.131 \times 10^{-1}$	$-7.647 \times 10^{-9}$	$-1.252 \times 10^{-3}$
5340.9	61.73	0.3131	62.53	$1.112 \times 10^{-1}$	$-3.278 \times 10^{-9}$	$-1.252 \times 10^{-3}$

### 3.2.3 The Numerical Model

The thermal response of the cylinders was modeled as one-dimensional transient heat

conduction with contact resistance at the interface. A description of the thermal contact resistance model for the interface is provided by Voth and Gill (1999). The transient, non-linear, turbulent, reacting flow, control volume code FVC (Blackwell et. al. 1998, Moen, 1999) was used to generate the model predictions. FVC allowed implementation of the contact conductance models described in Voth and Gill and because it also accommodates temperature dependent material properties.

The computation domain shown in Figure 3.1 was used for the numerical model. Note that the entire experimental apparatus was not modeled. The domain extends from TC2 to TC13 (see Table 3.1). The recorded temperature responses at these stations were used as time dependent boundary conditions for the model. Using the temperature measurements at these stations as boundary conditions reduces the uncertainties associated with contact resistance between the cylinders and the heating and cooling blocks. This allows one to focus on the contact resistance at the interface between the cylinders and the heat conduction within cylinders. Three uncertain model parameters were considered: the thermal conductivity, the volumetric heat capacity, and the contact conductance. Values for these model parameters are listed in Table 3.3 along with estimates of their standard deviations. The standard deviations were based on discussions with the experimentalist and were provided by Dowding (2000). The standard deviations represent 5% of the thermal conductivity, 2% of the volumetric heat capacity, and 10% of the contact conductance.

**Table 3.3: Model Parameters Statistics**

Parameter	Expected Value $\langle \alpha \rangle$	$\sigma$
$\alpha_1$ (thermal conductivity, $k$ )	15.06 W/m-C	0.753 W/m-C
$\alpha_2$ (volumetric heat capacity, $C$ )	$3.912 \times 10^6$ J/m <sup>3</sup> -C	$0.782 \times 10^5$ J/m <sup>3</sup> -C
$\alpha_3$ (contact conductance, $h$ )	1337.0 W/m <sup>2</sup> -C	133.70 W/m <sup>2</sup> -C

Model predictions using the model parameters listed in Table 3.3 were performed at Sandia National Laboratories and were provided to us by Dowding (2000). These are listed in Table 3.2. Also provided were estimates of the sensitivity coefficients of the predicted measurements to the parameters. In this report we use these sensitivity coefficients to construct an approximate model. The approximate model used here is based on the first few terms in a Taylor series expansion

$$\mathbf{T}(\boldsymbol{\alpha}) = \mathbf{m}(\boldsymbol{\alpha}) \approx \mathbf{m}(\langle \boldsymbol{\alpha} \rangle) + \mathbf{X}(\boldsymbol{\alpha} - \langle \boldsymbol{\alpha} \rangle) \quad (3.1)$$

where  $\mathbf{T}$  is the vector of approximate model predictions,  $\mathbf{m}(\boldsymbol{\alpha})$  is the functional

dependence of the model on the vector of model parameters  $\alpha$ ,  $\mathbf{m}(\langle\alpha\rangle)$  is the vector of the numerical model predictions using the expected value for the model parameters, and  $\mathbf{X}$  is the sensitivity matrix. As will be shown, the use of this approximate model with the validation methodology developed here gives comparable results to those obtained with the methodology developed previously (Hills and Trucano, 2001).

Figure 3.2 shows the predictions and the average measurements for the 10 data points as a function of time. Note that there are small discrepancies between the average measurements and the predictions. In Chapter 5, we will establish if these discrepancies are significant relative to the uncertainty defined by the parameter and the measurement uncertainty.

### 3.2.4 Probability Models for Measurements and Model Parameters

Asking the question – “Are the model predictions consistent with the experimental observations within the uncertainty of the experiment?” – requires the definition of models for this uncertainty. For the purpose of demonstration, we will assume that the underlying probability models for the model parameters and for the experimental observations are normally distributed. Other probability models will be considered for the shock physics example presented in the following section.

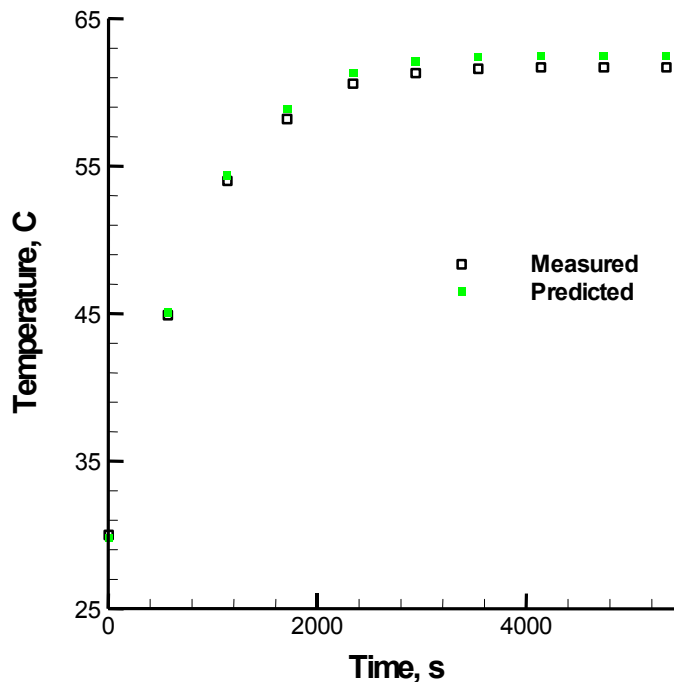


Figure 3.2: Temperature as a Function of Time

### 3.3 Impact of Aluminum on Aluminum

The second test case we consider is the symmetric impact of an aluminum plate upon an aluminum plate under conditions that guarantee that the resulting material response is in uniaxial strain (Hills and Trucano, 2001). Such impacts have been heavily modeled and well studied experimentally by the shock wave physics community. The experimental measurements for shock speed vs. particle speed are very repeatable and are consistent from experiment to experiment and from experimental technique to experimental technique. Figure 3.3 illustrates schematically the specific example of this type of impact that we care about here.

The resultant state of uniaxial strain is the most important part of the experiment, not the assumption that the materials are identical (which creates a significant simplification of the overall event as we will see). Uniaxial strain states, induced by such an impact, mean that the shock wave generated in the impact is a square-wave (at least in the ideal) and also guarantees that the resulting shock wave propagation can be analyzed as a one-dimensional Cartesian geometry wave propagation problem.

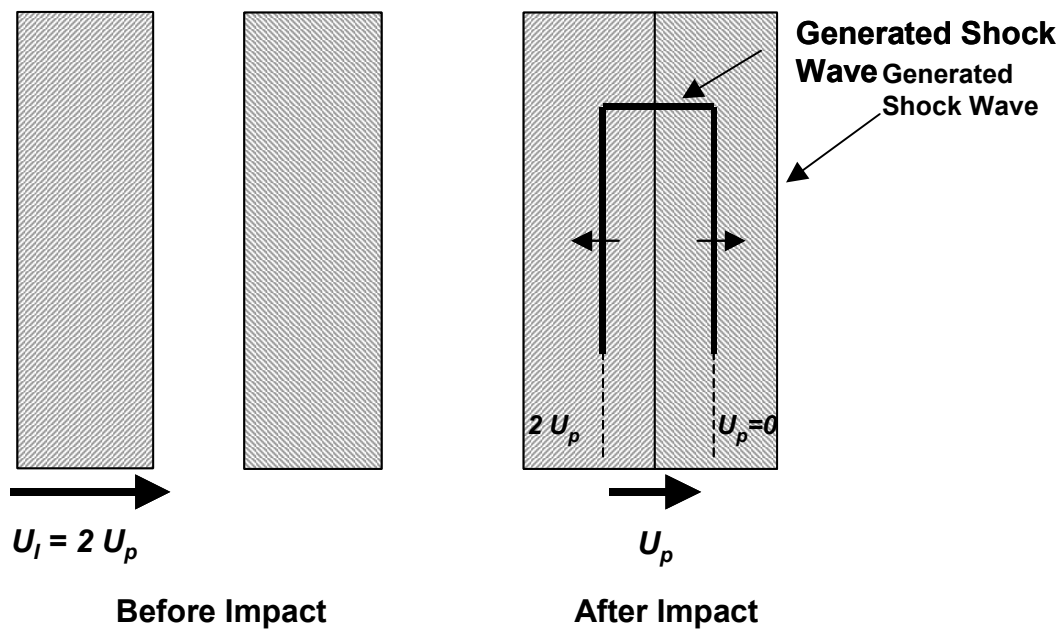
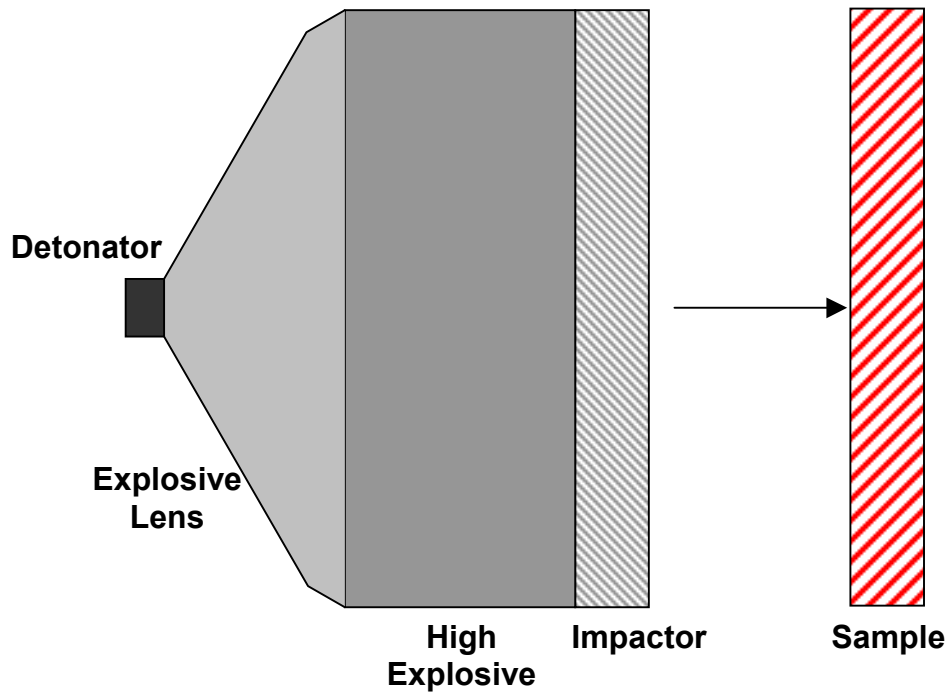


Figure 3.3: The Symmetric Impact of Two Aluminum Plates.

### 3.3.1 Experimental Data

The aluminum of specific interest in this report is 2024 aluminum. Our purpose is to compare a computational construction of the Hugoniot for this material with that reported experimentally in Marsh (1980). The Hugoniot of a material is the locus of thermodynamic states that is generated by the passage of a family of steady state shock waves of varying strength (Zel'Dovich and Raizer, 1967; Davison and Graham, 1979; Graham, 1993). Given the initial state and the shock velocity, the final state is uniquely determined. It is in this sense that the speed of the shock wave “parameterizes” the locus of Hugoniot states. Simple but important algebraic relationships between the shock wave speed and the initial and final states demonstrate the truth of this statement. These equations are called the *Rankine-Hugoniot conditions* (R-H).



**Figure 3.4: Explosive-Metal Geometry Feasible for Performing Shock Hugoniot Measurements.**

One approach for gathering shock wave data is depicted in Figure 3.4. The time of arrival of the shock wave at various points within or on the back of the sample, generated by the explosive configuration shown in Figure 3.4, was monitored through pin-contactors or

optical techniques (Rice, *et al.*, 1958; McQueen, *et al.*, 1970). This provided a measurement of shock speed  $U_S$ . These data also confirmed the planarity of the shock wave, a necessary condition for assumption of the uniaxial strain condition. In addition, the location of the rear surface of the sample was monitored (also through pin-contactors or optical techniques) to measure its free surface velocity upon breakout of the generated shock wave. The free surface velocity is the sum of the particle velocity due to the shock wave,  $U_P$ , and the particle velocity due to the resulting reflected rarefaction wave created by the intersection of the shock wave with the free boundary of the sample. Since each of these waves has approximately the same particle velocity (see Rice, *et al.*, 1958; McQueen, 1970), the free surface velocity is approximately twice the particle velocity  $U_P$ . Thus an estimate of the particle velocity is obtained from the free surface velocity measurement. Marsh (1980) described the approach that was used to correct for small inaccuracies in this method of particle velocity determination. By repeating the experiments using explosive systems designed to deliver different impact velocities, and hence different amplitude shock waves, the  $(U_S, U_P)$  points (hence density, pressure and internal energy of the material via the R-H conditions) on the Hugoniot curve are measured. While these data are not valid off the Hugoniot curve, they can be and are used to calibrate equation of state models for states near this curve (Rice, *et al.*, 1958).

### 3.3.2 The Measurement Data

Normally, model calibration data and model validation data are independent. In our case, we will use the  $(U_S, U_P)$  data from Marsh (1980) to calibrate the model and to test it. To provide some independence, we divide the data into two sets, one for calibration and one for model testing. The method used to divide the data depends on what one is trying to accomplish. For example, if we wish to test the ability of the model to extrapolate to higher values of  $U_P$ , we could use the  $(U_S, U_P)$  data in the low range to calibrate the model and use  $(U_S, U_P)$  data in the high range to test the model. The random process used to divide this set of data is discussed in Hills and Trucano (2001). Here we use the subsets of calibration and measurement data previously sampled in that report. The data selected for measurements are listed in Table 3.4 in the column labeled “ $U_S$  meas.”

We can either use prior knowledge of the uncertainty in the experimental technique to develop a probability model for the uncertainty in the measurements, or we can attempt to develop a probability model from the data directly. The second approach was used by Hills and Trucano (2001). They first used linear regression to remove the trend from the data. They then estimated the standard deviation of the residuals about the regression as an estimate for the uncertainty in the measurements. These residuals were tested using the Kolmogorov-Smirnov test to evaluate whether there was sufficient evidence to reject the

**Table 3.4: Predicted and Observed Shock Speeds (m/s)**

<i>Up</i>	<i>Us</i> meas	<i>Us</i> pred	<i>Us</i> resp	<i>Up</i>	<i>Us</i> meas	<i>Us</i> pred	<i>Us</i> resp	<i>Up</i>	<i>Us</i> meas	<i>Us</i> pred	<i>Us</i> resp
278	5811	5731.7	5731.3	1121	6840	6845.0	6842.9	2738	8916	8961.6	8960.7
440	6021	5946.5	5945.0	1128	6756	6852.1	6852.2	2817	9144	9060.7	9063.9
472	6054	5988.3	5987.1	1130	6823	6854.8	6854.8	2911	9070	9186.1	9186.7
503	5996	6030.1	6028.0	1134	6826	6860.2	6860.1	2935	9231	9211.4	9218.1
507	6055	6035.4	6033.3	1136	6831	6863.0	6862.7	2974	9236	9269.3	9269.1
609	6103	6170.0	6167.8	1141	6795	6869.7	6869.3	2987	9401	9285.4	9286.0
626	6262	6192.8	6190.2	1159	6915	6892.7	6893.1	3030	9177	9347.5	9342.2
627	6228	6194.1	6191.5	1220	6981	6974.4	6973.4	3031	9180	9348.2	9343.5
671	6164	6252.0	6249.6	1220	7014	6974.4	6973.4	3086	9317	9413.6	9415.4
722	6367	6319.4	6316.8	1277	6943	7047.5	7048.1	3181	9596	9540.0	9539.7
727	6323	6326.5	6323.4	1352	7092	7145.3	7146.4	3187	9549	9547.2	9547.5
728	6310	6327.9	6324.7	1383	7225	7187.8	7187.1	3217	9365	9592.5	9586.8
778	6388	6394.0	6390.7	1437	7156	7257.4	7257.9	3225	9666	9603.2	9597.3
786	6312	6403.1	6401.2	1446	7211	7270.1	7269.7	3238	9762	9614.2	9614.4
792	6314	6412.3	6409.1	1467	7305	7296.2	7297.2	3260	9477	9644.4	9643.2
792	6365	6412.3	6409.1	1498	7342	7339.6	7337.8	3274	9617	9655.6	9661.5
799	6353	6420.7	6418.3	1557	7462	7409.8	7415.1	3347	9775	9752.4	9757.2
800	6393	6422.1	6419.7	1574	7426	7438.4	7437.4	3361	9751	9781.7	9775.6
800	6459	6422.1	6419.7	1578	7326	7443.2	7442.7	3376	9803	9801.6	9795.2
802	6397	6424.8	6422.3	1605	7407	7479.1	7478.1	3381	9670	9807.6	9801.8
802	6355	6424.8	6422.3	1742	7690	7654.0	7657.6	3387	9609	9814.7	9809.6
809	6422	6433.2	6431.5	1744	7616	7659.3	7660.3	3400	9916	9828.9	9826.7
818	6366	6445.9	6443.4	1779	7758	7708.4	7706.1	3419	9866	9854.9	9851.6
831	6436	6461.8	6460.5	1858	7850	7809.0	7809.7	3463	9654	9901.4	9909.2
859	6470	6500.1	6497.5	1939	7773	7915.6	7915.8	3472	9697	9913.4	9921.0
863	6486	6505.3	6502.7	1948	7973	7927.8	7927.6	3481	9727	9931.5	9932.8
871	6561	6515.8	6513.3	1959	8015	7943.1	7942.1	3508	9861	9961.1	9968.2
888	6541	6537.8	6535.7	2154	8150	8199.8	8197.7	3508	9880	9961.1	9968.2
891	6589	6541.8	6539.7	2156	8332	8202.4	8200.3	3563	10117	10044.4	10040.3
896	6589	6547.0	6546.3	2335	8421	8432.7	8434.2	3629	10238	10127.7	10126.8
897	6579	6548.3	6547.6	2371	8436	8476.9	8481.2	3658	9876	10163.3	10164.8
901	6402	6553.7	6552.8	2467	8699	8602.9	8606.7	3736	10138	10273.5	10267.0
953	6616	6624.0	6621.4	2477	8618	8616.4	8619.7	3745	10162	10285.5	10278.8
953	6617	6624.0	6621.4	2595	8829	8771.9	8773.9	3772	10458	10315.1	10314.2
966	6659	6639.6	6638.6	2605	8744	8785.7	8787.0	3786	10341	10334.3	10332.5
975	6607	6652.1	6650.4	2608	8664	8789.9	8790.9	3930	10552	10524.0	10521.2
988	6507	6667.9	6667.6	2641	8848	8830.3	8834.0	3967	10384	10574.8	10569.7
1110	6844	6830.4	6828.4	2645	8797	8835.6	8839.2	3988	10572	10603.2	10597.2
1116	6843	6838.4	6836.4	2709	8792	8926.9	8922.8	4001	10572	10612.4	10614.3
1119	6846	6842.4	6840.3	2735	8909	8957.6	8956.8	4041	10572	10660.0	10666.7

residual as normally distributed. The test indicated that there was not sufficient evidence. As a result of this analysis, Hills and Trucano assumed that the measurement uncertainty was normally distributed, uncorrelated, with the following standard deviation:

$$\sigma_{meas} = 83.7 \text{ m/s} \quad (3.2)$$

The probability density function for a univariate normal distribution is given by

$$\text{PDF}_{\text{normal}}(x_n) = \frac{1}{\sqrt{2\pi}\sigma_{meas}} e^{-\frac{1}{2}\frac{x_n^2}{\sigma_{meas}^2}} \quad (3.3a)$$

where

$$x_n = \frac{d - \langle d \rangle}{\sigma_{meas}} \quad (3.3b)$$

and  $d$  and  $\langle d \rangle$  represent the measurement and the expected value of the measurement. We will estimate  $\langle d \rangle$  as part of the model validation process in the following chapters.

We will also consider a second, more complex model for the measurement uncertainty to demonstrate the application of the present methodology to non-normal distributions. For illustrative purposes, we arbitrarily assume that the measurement uncertainty is distributed as a Beta distribution (Miller and Freund, 1985) with a width  $d_{ub} - d_{lb} = 6 \sigma_{meas}$  (see (3.2)), and the Beta distribution parameters  $b_1=3$  and  $b_2=2$ . The Beta distribution is a finite width distribution with upper and lower bounds denoted by  $d_{ub}$  and  $d_{lb}$ . The Beta distribution was chosen because it can model a wide variety of statistical data. For example, if  $b_1=b_2$ , the distribution is symmetric. Further, if  $b_1=b_2=1$ , the distribution reduces to a uniform distribution. The probability density function for this distribution is given by

$$\text{PDF}_{\text{beta}}(x_b) = \begin{cases} \frac{\Gamma(b_1 + b_2)}{\Gamma(b_1)\Gamma(b_2)} x_b^{b_1-1} (1 - x_b)^{b_2-1}, & 0 < x_b < 1 \\ 0, & \text{otherwise} \end{cases} \quad (3.4a)$$

where

$$x_b = \frac{d - d_{lb}}{d_{ub} - d_{lb}} \quad (3.4b)$$

### 3.3.3 The Model Parameters

We recall the general quadratic functional form of the  $(U_S, U_P)$  Hugoniot relationship (Hertel and Kerley, 1998):

$$U_S = C_S + S_1 U_P + (S_2 / C_S) U_P^2 \quad (3.5)$$

where  $C_S$ ,  $S_1$ , and  $S_2$  are calibration constants based on  $(U_S, U_P)$  data. As discussed in Hills and Trucano (2001), the aluminum data of concern here are well modeled by a linear relationship. Because of this, we set the constant on the quadratic term in Eq. (3.5) to zero

$$S_2 = 0 \quad (3.6)$$

and use least squares to estimate the intercept,  $C_S$ , and the slope,  $S_1$  as well as the covariance matrix for these parameters. The resulting regression coefficients and their statistics are listed in Table 3.5. Details of this regression analysis is presented in Hills and Trucano (2001). Note that we show the two coefficients as components in the model parameter vector  $\alpha$ .

**Table 3.5: Calibration Constants**

	Coefficient	Covariance Matrix	
		$\alpha_1$	$\alpha_2$
$\alpha_1 (C_S)$	5344	166.4	-0.0663
$\alpha_2 (S_1)$	1.305	-0.0663	3.50 E-5

Hills and Trucano (2001) investigated the normality of the residuals associated with the calibrated model. They found no significant evidence to reject the hypothesis that these are normally distributed. Here we will assume two models for the uncertainty in these parameters. The first is based on a multinormal distribution, with the expected values and the covariance as listed in Table 3.5. The corresponding multivariate probability density function for this model is defined by

$$\text{PDF}(\alpha) = \frac{1}{\sqrt{(2\pi)^n |\mathbf{V}_\alpha|}} \exp(-(\alpha - \langle \alpha \rangle)^T \mathbf{V}_\alpha^{-1} (\alpha - \langle \alpha \rangle)) \quad (3.7)$$

where  $\alpha$  and  $\langle \alpha \rangle$  are the vectors of model parameters and their expected values, and  $\mathbf{V}_\alpha$  is the covariance matrix.

The second probability model we consider is based on a normal distribution for  $\alpha_1$  and a triangular distribution for  $\alpha_2$ . We arbitrarily chose these distributions to illustrate the application of the methodology developed here for more general multivariate distributions. The normal distribution for  $\alpha_1$  is given by

$$\text{PDF}_{\text{normal}}(x_n) = \frac{1}{\sqrt{2\pi}\sigma_{\alpha_1}} e^{-\frac{1}{2}x_n^2} \quad (3.8a)$$

where

$$x_n = \frac{\alpha_1 - \langle \alpha_1 \rangle}{\sigma_{\alpha_1}} \quad (3.8b)$$

The triangular distribution assumed for  $\alpha_2$  is given by

$$\text{PDF}_{\text{triangular}}(x_t) = \begin{cases} 4x_t, & 0 < x_t \leq 0.5 \\ 4(1-x_t), & 0.5 < x_t \leq 1.0 \\ 0, & \text{otherwise} \end{cases} \quad (3.9a)$$

where

$$x_t = \frac{\alpha_2 - \alpha_{2-lb}}{\alpha_{2-ub} - \alpha_{2-lb}} \quad (3.9b)$$

The mean and standard deviation for the normal distribution are based on those for  $\alpha_1=C_s$  listed in Table 3.5. Standard deviation is the square root of the (1,1) element in the covariance matrix. The lower and upper bounds for the triangular representation of the uncertainty in  $\alpha_2=S_I$  are based on plus or minus three standard deviations of the corresponding values from Table 3.5. Note that for this example, we assumed that there is no correlation between the model parameters or between the measurements. A summary of the distributional parameters for the alternate probability models is listed in Table 3.6.

**Table 3.6: Distribution Parameters for Alternate Probability Models**

Variable	Distribution	Parameter	Value
$\alpha_1$ (Cs)	Normal	$\langle \alpha_1 \rangle$	5344 m/s
		$\sigma$	12.90 m/s
$\alpha_2$ (S1)	Triangular	$\alpha_{2-lb}$	1.287
		$\alpha_{2-ub}$	1.323
<b>d</b>	Beta	$d_{ub}-d_{lb}$	502.2, m/s
		$b_1$	3.0
		$b_2$	2.0

### 3.3.4 The Physical Model

Our approach to the model calculation is fully defined in Figure 3.3 and is thus a simplification of the actual experiment as we suggested above. Our computations will treat each experimental ( $U_S$ ,  $U_P$ ) point as having been generated by an appropriate symmetric impact of 2024 aluminum on 2024 aluminum. This simplified “experiment” is defined by an impact velocity  $U_I$  that is twice the reported particle velocity for the specific data point given in Marsh’s compendium.

For example, a particle velocity of 278 m/s is the smallest reported in Table 3.4. The corresponding impact velocity of 556 m/s is required for the symmetric impact that should reproduce this data point. Similarly, 4.041 km/s is the highest reported value of particle velocity, and an impact velocity of 8.082 km/s is required to reproduce this point. The R-H relations can be used to determine that the lowest impact velocity in the data we analyze produces a shock wave having a pressure of approximately 44 kbars, which is a factor of more than fourteen times the yield stress of 2024 aluminum. In this case, therefore, we accept without further discussion that the aluminum can be accurately modeled as a fluid rather than as an elastic solid. The equation of state of the aluminum thus becomes the only important constitutive description in the problem. At all other data points in Table 3.4 the pressure is higher, so this modeling assumption is made for the entire range of data that we discuss.

We use the Sandia Eulerian shock wave physics code CTH (McGlaun, et al, 1990; Bell et. al., 1998) to simulate the one-dimensional impact of 2024 aluminum on 2024 aluminum illustrated in Figure 3.3. This model, including details of its implementation, is discussed further in Hills and Trucano (2001).

**Table 3.7: Interpolation Table of Shock Speed as a Function of Particle Speed and Model Parameters**

$U_p$ , m/s	$C_s$ , m/s	$S_I$	$U_s$ , m/s	$U_p$ , m/s	$C_s$ , m/s	$S_I$	$U_s$ , m/s
250.0	5237.120	1.2528	5574.299	2175.0	5379.626	1.2528	8146.057
250.0	5237.120	1.2876	5584.302	2175.0	5379.626	1.2876	8226.924
250.0	5237.120	1.3224	5591.328	2175.0	5379.626	1.3224	8296.186
250.0	5237.120	1.3572	5600.016	2175.0	5379.626	1.3572	8374.474
250.0	5308.373	1.2528	5645.378	2175.0	5450.879	1.2528	8222.766
250.0	5308.373	1.2876	5654.100	2175.0	5450.879	1.2876	8291.586
250.0	5308.373	1.3224	5662.542	2175.0	5450.879	1.3224	8367.459
250.0	5308.373	1.3572	5672.953	2175.0	5450.879	1.3572	8442.861
250.0	5379.626	1.2528	5717.530	3137.5	5237.120	1.2528	9215.381
250.0	5379.626	1.2876	5726.257	3137.5	5237.120	1.2876	9329.407
250.0	5379.626	1.3224	5734.736	3137.5	5237.120	1.3224	9426.386
250.0	5379.626	1.3572	5743.242	3137.5	5237.120	1.3572	9530.964
250.0	5450.879	1.2528	5788.653	3137.5	5308.373	1.2528	9288.138
250.0	5450.879	1.2876	5797.378	3137.5	5308.373	1.2876	9398.135
250.0	5450.879	1.3224	5805.858	3137.5	5308.373	1.3224	9490.674
250.0	5450.879	1.3572	5814.594	3137.5	5308.373	1.3572	9605.582
1212.5	5237.120	1.2528	6795.464	3137.5	5379.626	1.2528	9362.063
1212.5	5237.120	1.2876	6836.658	3137.5	5379.626	1.2876	9466.073
1212.5	5237.120	1.3224	6876.047	3137.5	5379.626	1.3224	9575.774
1212.5	5237.120	1.3572	6917.521	3137.5	5379.626	1.3572	9675.540
1212.5	5308.373	1.2528	6866.484	3137.5	5450.879	1.2528	9430.747
1212.5	5308.373	1.2876	6905.983	3137.5	5450.879	1.2876	9541.455
1212.5	5308.373	1.3224	6948.932	3137.5	5450.879	1.3224	9642.970
1212.5	5308.373	1.3572	6988.025	3137.5	5450.879	1.3572	9742.838
1212.5	5379.626	1.2528	6939.142	4100.0	5237.120	1.2528	10423.750
1212.5	5379.626	1.2876	6979.220	4100.0	5237.120	1.2876	10573.920
1212.5	5379.626	1.3224	7020.266	4100.0	5237.120	1.3224	10697.530
1212.5	5379.626	1.3572	7061.384	4100.0	5237.120	1.3572	10849.030
1212.5	5450.879	1.2528	7008.270	4100.0	5308.373	1.2528	10502.210
1212.5	5450.879	1.2876	7052.366	4100.0	5308.373	1.2876	10639.890
1212.5	5450.879	1.3224	7093.119	4100.0	5308.373	1.3224	10774.770
1212.5	5450.879	1.3572	7131.756	4100.0	5308.373	1.3572	10916.260
2175.0	5237.120	1.2528	8009.234	4100.0	5379.626	1.2528	10580.560
2175.0	5237.120	1.2876	8079.695	4100.0	5379.626	1.2876	10706.400
2175.0	5237.120	1.3224	8148.098	4100.0	5379.626	1.3224	10854.930
2175.0	5237.120	1.3572	8229.619	4100.0	5379.626	1.3572	10972.300
2175.0	5308.373	1.2528	8079.459	4100.0	5450.879	1.2528	10646.880
2175.0	5308.373	1.2876	8152.193	4100.0	5450.879	1.2876	10781.010
2175.0	5308.373	1.3224	8225.404	4100.0	5450.879	1.3224	10913.500
2175.0	5308.373	1.3572	8294.047	4100.0	5450.879	1.3572	11052.840

A response surface approach was used to represent the behavior of the model over the range of parameters. Specifically, CTH was used to evaluate  $U_s$  on a 4x4x5 grid of  $C_s$ ,  $S_I$ ,  $U_p$  values, respectively. Trilinear interpolation was then used to evaluate  $U_s$  throughout the grid. The grid values are listed in Table 3.7. The response of  $U_s$  is well modeled by linear interpolation on  $C_s$ ,  $S_I$ ,  $U_p$  over the range of values shown in the table (see Hills and Trucano, 2001). A more nonlinear response would require a denser grid for trilinear interpolation, or a higher order interpolating function, or both.

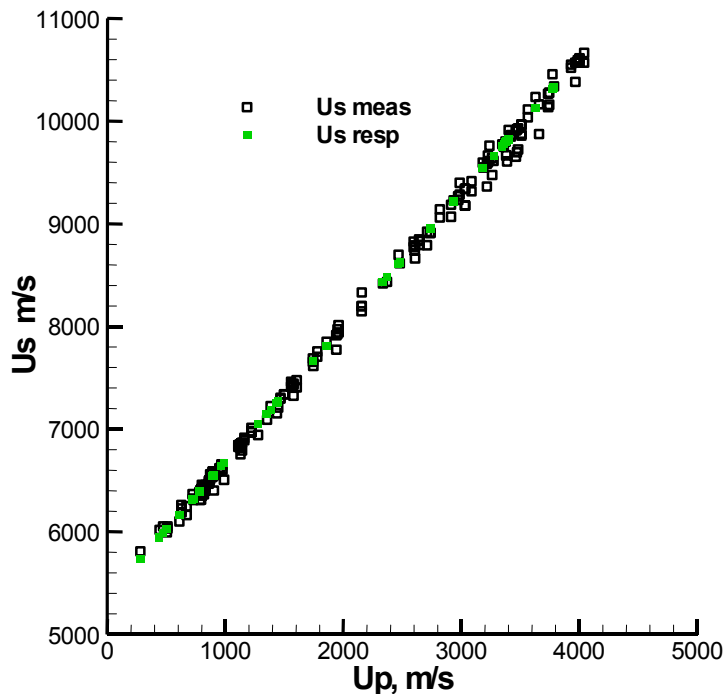


**Figure 3.5: Predicted and Observed Shock Speeds as a Function of Particle Speed: The predicted speeds are based on tri-linear interpolation using the values of Table 3.7**

Table 3.4 gives 120 particle velocities of the measurements, the measured shock speed, the predicted shock speed using CTH directly, and the predicted shock speed using the response surface representation at the mean model parameters listed in Table 3.5. Note that the agreement between the direct CTH predictions and the response surface predictions is very good and the response surface does indeed model the numerical

response well. This is not surprising considering that the model is linear in the parameters, for this particular application, over this particular range of particle velocities. A plot of the predicted shock speed using the response surface evaluated at the mean values of the parameters and the experimental data is presented in Figure 3.5. The results show that the predicted and measured shock speeds agree well. We will next evaluate whether there is statistical evidence that the agreement is good relative to the modeled uncertainty in the model validation exercise.

## 4.0 Maximum Likelihood Method

### 4.1 Introduction

In the previous work by Hills and Trucano (1999, 2001), the uncertainty in the model predictions was added to the uncertainty in the experimental observations to obtain a total uncertainty for the differences between the model predictions and the experimental observations. While this approach is conceptually simple, it can be computationally expensive since we must numerically generate  $n$ -dimensional surfaces describing the constant probability density function (PDF) surfaces to define cumulative probability. While the generation of such surfaces is straight forward for predictions and observations that are both normally distributed, the approach is more difficult when the predictions and observations are modeled by different distributions. For nonlinear problems, the probability distribution for the predictions can be non-normal, even though the distributions for the model parameters are normal.

In the present work, we take a different approach. Rather than defining the entire PDF cloud for the  $n$ -dimensional space and then evaluating the probability of a model prediction/experimental observation, we use optimization to search through this space to find the point of maximum likelihood of the joint PDF. As in the previous work (Hills and Trucano, 1999, 2001), we focus on two sources of uncertainty; 1) the uncertainty in the measurements, and 2) the uncertainty in the model parameters. We assume that the uncertainty in the measurements and the uncertainty in the model predictions are independent.

The joint probability density function of a particular measurement vector  $\mathbf{d}$  occurring, and a particular model parameter vector  $\boldsymbol{\alpha}$  occurring, is given by the products of the individual probability densities:

$$\text{PDF}(\mathbf{d}, \boldsymbol{\alpha}) = \text{PDF}(\mathbf{d}) \text{PDF}(\boldsymbol{\alpha}) \quad (4.1)$$

It is important to note that this joint probability density function is not necessarily the same as the joint PDF of the observations and the model predictions:

$$\text{PDF}(\mathbf{d}, \mathbf{p}) = \text{PDF}(\mathbf{d}) \text{PDF}(\mathbf{p}) \quad (4.2)$$

This difference is significant and we will return to this point at the end of this chapter.

Given a set of experimental measurements and a model for their uncertainty, and a set of mean model parameters and a model for their uncertainty, we wish to evaluate the probability that the model is consistent with the observations and the parameter uncertainty. There are two problems that we face:

1. While we have a statistical model for the model parameters that includes some measure of central tendency (i.e., mean, expected value, or mode) and spread (i.e., variance or min-max), we don't know the actual values of the model parameters  $\alpha$  for this particular realization of the validation experiment.
2. In general, we wish to include the case of only one realization of the experiment in our development. Thus, we have only one realization of the measurement vector and we need to somehow estimate something about the true values of the measurements.

Here our approach is to use maximum likelihood to estimate the most likely value for the model parameter vector; for this particular realization of the validation experiment, and given that the model is valid. We then evaluate the probability that such parameters are obtained for a valid model. The assumptions made in applying this approach are as follows:

1. We assume that the measurements are independent of the model parameters. We also assume that the measurement distribution has one peak and is thus unimodal.
2. The model for the uncertainty in the model parameters is correct.
3. The functional form of the uncertainty in the measurements is correct. Our measure of spread has the correct value (i.e., standard deviation, max-min).
4. We expect the model to provide predictions that agree with the mode (i.e., the location of maximum probable density) of the measurements, if the model is valid and if the true values of the model parameters are used. The approach can be easily changed to use the expected value or median rather than the mode.

We will show later that this method is equivalent to the methods applied in previous work (Hills and Trucano, 1999, 2001) for models locally linear in the model parameters and for model parameters and measurements that are normally distributed.

## 4.2 Geometry

We now consider the geometric interpretation of this approach. A similar interpretation is presented in Hills and Trucano (2001) for the previous developed metrics. Here we extend this interpretation to explicitly account for the subspace spanned by the model.

For the purpose of this discussion, assume that we have 3 measurements,  $\theta_1$ ,  $\theta_2$ , and  $\theta_3$ . We also assume that we have a model that predicts these 3 measurements and is based on the 2 parameters  $\alpha_1$  and  $\alpha_2$  that contain significant uncertainty. The corresponding validation space is shown in Figure 4.1. Note that we are defining the space using the 3 measurements. These could be measurements taken from different locations or measurements taken at the same location at different times, or a combination of both. This space can easily be generalized to  $n$  measurements and  $m$  parameters by considering an  $n$ -dimensional space. Note that for the case illustrated in Figure 4.1, we have more measurements than we have model parameters. Thus, our model is restricted to a subspace of the measurement space. In this case, our model's dependence on the uncertain parameters is represented as a 2 dimensional surface in the 3 dimensional space. Also shown in the figure are probability density function clouds for the measurements, the model parameters, and the uncertainty in the model predictions due to the uncertainty in the model parameters. For the case for which we have a 1-1 mapping between the model predictions on the 2 dimensional surface and the values of the parameters, we can assign a  $\alpha_1$  -  $\alpha_2$  pair to each location on the model surface as shown in the figure. However, the 1-1 mapping is not a requirement of the present approach.

We now consider the geometric interpretation from a model validation perspective. Figure 4.1 shows a vector of measurements that does not lie on the model surface. For the case of more measurements than model parameters, we would expect the measurement to lie off the model surface due to measurement error. If we have more model parameters than measurements, then this may not be the case – i.e., there may be enough degrees of freedom in the model parameters to fit the model exactly to the measurements. However, the fit may require that the parameters be chosen from regions of low probability – i.e., chosen on the fringes of the PDF clouds for the model predictions and the model parameters. This would cast doubt on the validity of the model.

In general, the measurements will lie off the model surface when we have more measurements than uncertain parameters, even if the model is valid. We now ask the question – what relationship must hold between the measurement cloud and the prediction cloud if the model is correct? We make the following observations:

1. We really don't know what the true values of the model parameters are for this realization of the validation experiment. We do have a model for the expected

values of the parameters and for the probability distribution. We can, in principle, propagate this through the model to obtain the corresponding model for the uncertainty (PDF cloud) on the model prediction surface as shown in Figure 4.1. If we know the true values of the parameters for this realization of the experiment, then our model prediction would be a point somewhere on the prediction surface within the PDF prediction cloud.

2. We really do not know the true value of the measurement vector. We only know what we observed and that our observations contain errors of the assumed form. The true value is probably at some other location in the validation space – perhaps on the model surface.

So what do we expect out of a valid model and the corresponding measurements? We would like the true value of the measurement vector to equal the model predictions using the true value of the parameters. Unfortunately, we know neither the true values of the measurements nor the true values of the parameters. We do know (or assume we know) the expected value of the model parameters, and we have one observation of the measurement vector with the associate uncertainty. However, we don't know the expected value of the measurement vector. In terms of Figure 4.1, we don't know the location of the cloud in the validation space. We just know that it contains the measurement.

Here we assume that if we were somehow able to repeat the experiment many times, without varying the true values of the model parameters (for example – use the same test specimen over and over), then the model predictions of the measurements for a valid model using the true parameter values would be equated to some measure of central tendency of the resulting measurement distribution. The choice of the measure of central tendency is somewhat arbitrary. Here we choose to use the mode, which is the location in the measurement distribution that is most likely – i.e., where the probability density function has a maximum. We could also use the median or the expected value. In fact, these three measures of central tendency are equivalent if the distribution is symmetric. Based on this choice, we expect the mode of the measurement vector to lie on the model surface of Figure 4.1 for a valid model. For the symmetric measurement distribution shown in Figure 4.1, the mode is at the center of the measurement PDF and should lie on the model surface. Clearly, the mode (or any other measure of central tendency for the distribution) does not lie on the model surface for the case shown in Figure 4.1. We would thus have to question the validity of the model illustrated in the figure based on this measure.

Our approach is to estimate the maximum likely values for the mode of the measurement vector and the true model parameters, assuming that the model is valid. We then evaluate the probability of these values for a valid model. If the probability is small, we question the validity of our model.

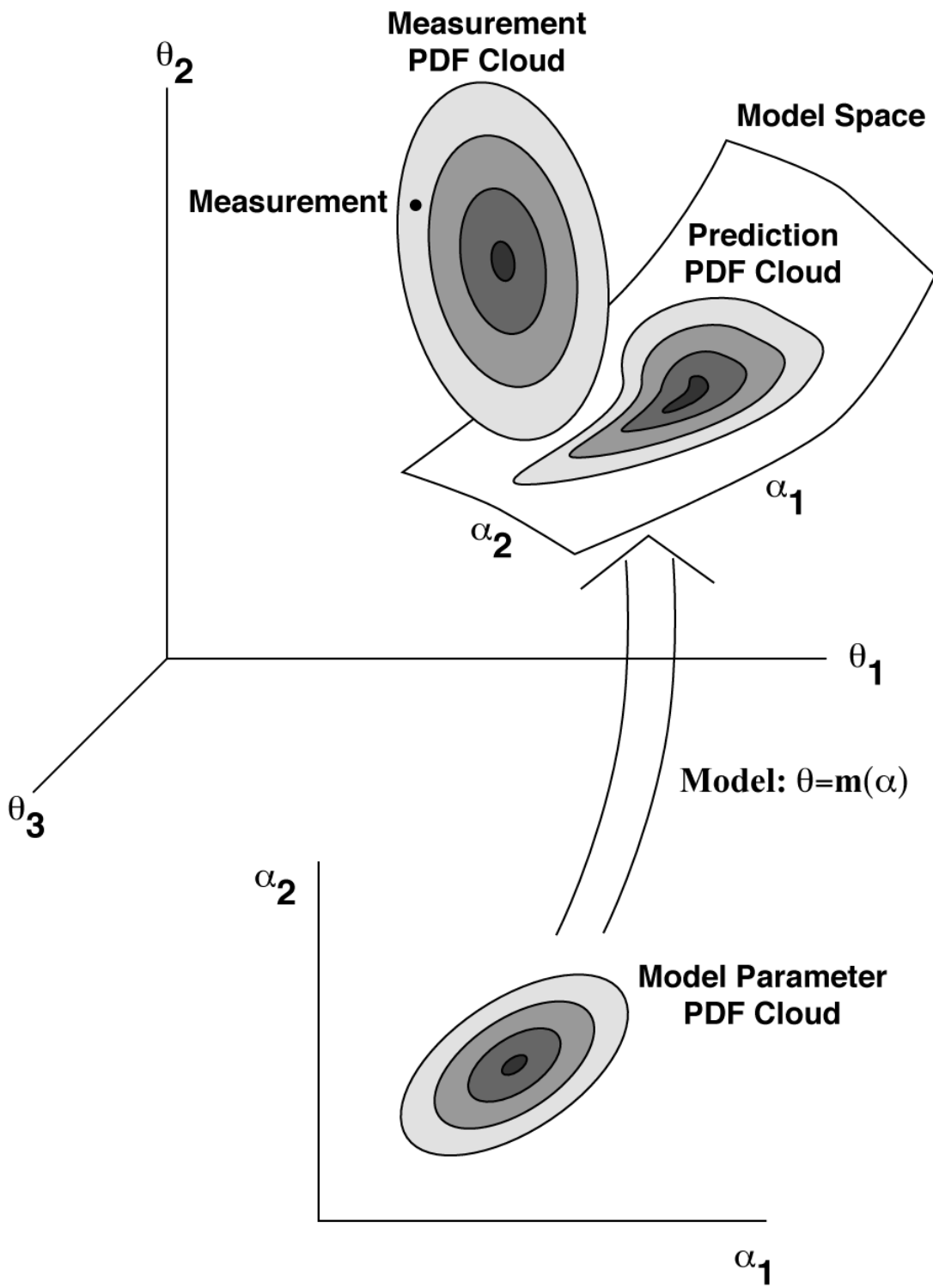


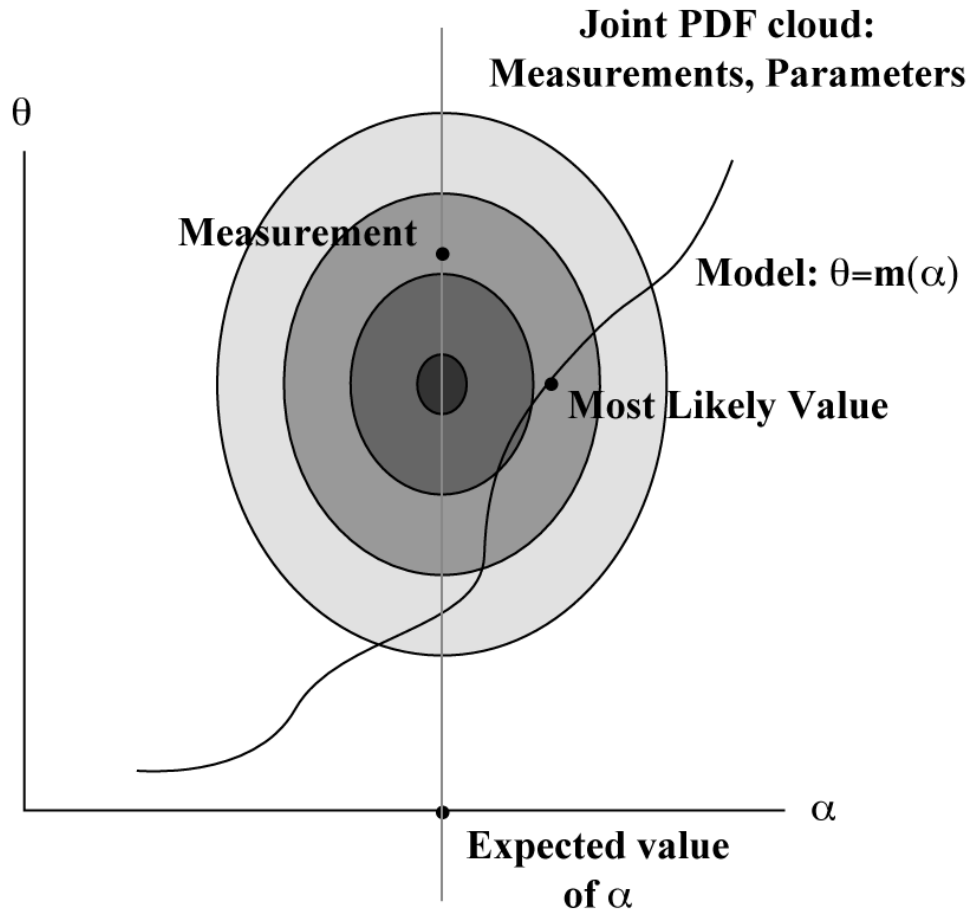
Figure 4.1: Geometry of the proposed validation metric.

Figure 4.2 shows another graphical interpretation of the maximum likelihood process. Here we add dimensions to the space of Figure 4.1 to represent the model parameters shown. For the 3 measurements and 2 model parameter case, we would actually have a 5 dimensional space. For this case, the model appears as a 2 dimensional surface that runs through 5 dimensional space. We now show a joint PDF cloud in terms of the model parameters and the measurements. Again we assume that the expected value for the parameter distribution is known. The center (for a symmetric cloud) of the cloud should thus lie on the vertical line. We don't know where on this line it lies, since we don't know the mode (or expected value or median) of the measurements. However, we will estimate this location and the location of the true values of the model parameters, such that the resulting estimates are most likely, given the experimental data. Since we are assuming that the modes of the measurements are equal to the model predictions, when we use the true values for the model parameters, we must have that both of these lie at the same values for  $\theta$  as shown in Figure 4.2. To estimate the values of the true parameters, we move the PDF cloud up and down along the vertical line such that the joint probability of the true values for the model parameters and the experimental observations is maximized. Note that as the PDF cloud is moved down, the point at the same  $\theta$  on the model surface moves closer to the center of the PDF cloud, increasing the PDF value for the corresponding model prediction. However, as the cloud moves down, the experimental measurements are now in a location of lower PDF. Since we are interested in the joint PDF, the optimum location for the cloud will lie somewhere in between. Once we establish the location of the cloud, we can then evaluate the probability of obtaining this set of parameters and this set of measurements for a valid model.

### **4.3 Maximum Likelihood Procedure**

Any suitable optimization routine can be used to find the maximum likelihood values for the location of the cloud. A function evaluation routine must be provided to the optimization routine, which evaluates the objective function given a guess for the parameter vector  $\alpha$ . Here the function evaluation routine should do the following:

1. Given the vector of parameters  $\alpha$ , evaluate the corresponding predictions, which we are assuming are equal to the mode of the measurements. This locates the PDF vertically in Figure 4.2.
2. Given the vector of parameters  $\alpha$  and the vertical location of the PDF, evaluate the joint probability density of the measurements and the parameters using Eq. 4.1. Since most optimization routines minimize rather than maximize, return the negative of the joint probability density to the calling optimization routine.



**Figure 4.2: Maximum Likelihood Estimate**

This procedure is fairly straightforward and we will provide more details on the process in the following chapter.

#### **4.4 Significance of the Estimated Parameters**

Once we have evaluated the parameter values using the procedure described above, we must evaluate the probability of obtaining these values for a valid model. The above procedure provides the most likely values for the model parameters and for the modes of the measurements; given the observed measurements, and given that the model is correct. In evaluating the parameters, we applied the constraint that the model predictions, using the estimated true values of the parameters, are consistent with the mode of the measurement distributions. We searched through the space of parameters to find those parameter values that result in the maximum joint probability density, given the constraint

that the model predictions (using the true value of the model parameters) agree with the mode of the measurements. We now ask the question – what is the probability of obtaining a lower value for PDF given a valid model?

For PDFs that are normally distributed, this question can be answered quite easily since we can use the  $\chi^2$  distribution (Beck and Arnold, 1977; Hills and Trucano, 2001). We will show this special case for several of the examples that are presented in the following chapter.

If we are dealing with more complex distributions or joint distributions of several kinds (a normal, triangular, and Beta, for example), we will evaluate the probabilities numerically. This process is surprisingly straight forward if we use a Monte Carlo approach. The process is as follows:

1. Generate a random number for each of the distributions (i.e., for each parameter and each measurement) and evaluate the corresponding joint probability density (i.e., the products of the individual probability densities if the random variables are independent). The spread of the distributions should be the same as those used for the maximum likelihood process described above. The locations of the distributions don't matter (i.e., its mean, mode, or median) since we are really only interested in the probability density of the random number, not its value.
2. Repeat this process many times and count the number of times the joint probability density is less than that obtained from the maximum likelihood process.

The percentage of the time that the value for the probability density obtained from this Monte Carlo process is smaller than that obtained from the optimization procedure, represents an approximation to the cumulative probability that a valid model would have a PDF less than that estimated. Here we refer to this cumulative probability as the significance. If this significance is small, then the probability that a valid model would produce the observed differences between measurement and prediction is small and we would have little confidence in the model. Note that the Monte Carlo procedure does not require any evaluations of the predictive model. It simply requires the generation of random numbers, the evaluation of the joint probability density of these numbers, and the count of the number of times the joint probability density is less than that already obtained from the optimization process. Because of this, the Monte Carlo process requires little CPU resources.

We will illustrate the Monte Carlo approach for the shock physics application using the mixture of distributions described in Sections 3.3.2 and 3.3.3.

## 4.5 Discussion

At first glance, the maximum likelihood procedure described above is suspiciously similar to model calibration. In fact, the procedure used here is a form of model calibration - one that uses some prior knowledge of the model parameter distributions and the measurement distributions to estimate the parameters. This methodology then takes an important additional step. It asks the question – what is the significance of the estimated model parameters and the observed measurements, given a valid model? If this significance is small, then we have sufficient evidence to question the validity of the model. What we are really doing is using a maximum likelihood procedure to estimate the model parameters, and then asking the question – are these parameters reasonable given what we know about their distributions and those of the measurements?

Note that this approach contrasts with model calibration when we have no prior knowledge of the parameters. For example, if we were to use ordinary least squares to fit the model to the measurements, then the parameter values that would be chosen would have a residual vector (difference between the model predictions using these parameter values and the experimental observations) that is orthogonal to the model surface shown in Figure 4.1. In other words, if we were to project the measurement shown in Figure 4.1 down onto the model surface, then this would be our nonlinear, ordinary least squares estimate of the model parameters. We are forcing the model to best fit the experimental data, regardless of the probability density of the parameters. However, as Figure 4.1 suggests, the resulting model parameters may be near the edge of the prediction PDF suggesting that such parameters are unlikely. If we then ask the question – are these parameters and measurements likely? – then we could use the significance of these parameters and measurements as a *metric* of model validity.

Our present approach is really asking a different question than that asked in the previous work by Hills and Trucano (2001). Here we ask what the significance is of a set of observed measurement and calibrated model parameters, given a valid model and the probability distributions for the measurements and the parameters. If the significance is small, then we have good reason to suspect the validity of the model. The approach used previously by Hills and Trucano evaluated the significance of obtaining the observed differences in the model predictions and the experimental observations. Both of these metrics are appropriate measures to evaluate the validity of a model. In fact, the metrics obtained by the two approaches will be the same for the normal distributions considered by Hills and Trucano when coupled with a sensitivity analysis used to propagate parameter uncertainty through the model. We will show this equivalence in Chapter 6.

This above represents an approach to defining model validation metrics that are based on the physical model and the models for the uncertainty in the measurements and in the model parameters. We are in-fact making several underlying assumptions in this approach. These are:

1. The use of a statistical metric based on joint probability is an appropriate metric. We are assuming that the use of a statistical metric based on joint probability is appropriate rather than some other metric, such as the maximum difference between a model prediction and the measurements. The advantage of this approach is it forces us to quantify the overall uncertainty in the validation exercise, which in-turn allows us to evaluate whether the uncertainty in the validation exercise is sufficiently small relative to the acceptable level of uncertainty in the anticipated application. Once we decide to measure model validity in terms statistical consistency with the data, then the form of the validation metric is by the validation exercise uncertainty.
2. The underlying distributions for the uncertainty in the measurements and the model parameters are correct. Since the definition of our metric follows directly from the form of the models for uncertainty in the model parameters and in the measurements, our validation metric assumes that these models are correct. If we find that the model predictions are not consistent with the experimental observations, then all we can really say is that the physical model, coupled with the statistical models for uncertainty, are not consistent with the data. So, we are really testing the models for uncertainty as well as the physical model.
3. A valid model's predictions, using the true value for the model parameters for a validation exercise, is equal to the value obtained for some measure of central tendency of the uncertainty in the measurements. For example, if our measurement at some location and time is normally distributed due to uncertainty, then we are assuming that if we repeat this experiment many times, using the same experimental apparatus (such that the model parameters don't change), the distribution of the measurements at this location and time is centered on a valid model's prediction. The choice of what measure of central tendency to use on the measurements becomes more arbitrary for non-symmetric distributions. We could choose the mean, mode, or median. Judgment on which measure of central tendency to use depends on the type and quality of data used to define the measurement uncertainty.
4. The true values of the model parameters are the maximum likely values, given the joint PDF for the measurements and the model parameters, and the assumptions defined in items 1-3 above. The use of maximum likelihood approach is well accepted (see Beck and Arnold, 1977) when dealing with nonlinear systems and non-normal distributions. As will be shown in a latter chapter, this approach, and the non-optimization

approach developed in Hills and Trucano (1999, 2001) give the same metric for locally linear models with normally distributed model parameters.

5. Finally, if we define a threshold of significance below which the model is considered invalid, say at the 5% level, then we have basically assumed that we have a reason to use this value for the threshold. Traditionally, statisticians use threshold values for the level of significance as 10%, 5%, 2%, or 1% in statistical inference. The choice of which threshold to use is based on the trade-off between the probability of committing a Type I error – rejecting a good model, and the probability of committing a Type II error – failing to reject a bad model. As one provides more benefit of doubt to the model, i.e. uses a smaller threshold, one also increases the chances of failing to reject a bad model. Ideally, the choice of the level of significance should be tied to the anticipated application of the model, the cost of accepting a bad model, and the cost of rejecting a good model. For example, if the model validation experiments are performed over the same range of conditions as the anticipated application, and a bad model performs well over this range, then the cost of not rejecting this model may be small since this model was found to represent the application over the anticipated range of conditions. We need to develop methodology to relate the results of our validation experiments to the predictions of our anticipated application. This will help to clarify the relation of threshold significance in the validation experiments to acceptable uncertainty in the anticipated application. Such work is anticipated in the near future.

(Page left blank)

## 5.0 Applications

### 5.1 Introduction

We are now ready to demonstrate this maximum likelihood approach outlined in the previous chapter to the applications introduced in Chapter 3. We begin with the heat conduction problem.

### 5.2 Application to the Heat Conduction Data

As discussed in Chapter 3, we assume that the PDF for the uncertainties in the measurements and in the model parameters are normally distributed with the statistics listed in Tables 3.2 and 3.3.

We are now ready to estimate the most probable values for the mode of the measurements  $\mathbf{d}$  and the model parameters  $\boldsymbol{\alpha}$ . The mode for the PDF in the measurements is equal to the expected value of  $\mathbf{d}$  for a symmetric distribution, such as the normal distribution considered here. So in this case, we can equivalently estimate  $\langle \mathbf{d} \rangle$  and the  $\boldsymbol{\alpha}$  that has maximum joint likelihood, subject to the constraint imposed by the model. The joint PDF of the model parameters and the experimental data for our normal distributions is given by (see Beck and Arnold, 1977)

$$\begin{aligned} \text{PDF}(\mathbf{d}, \boldsymbol{\alpha}) &= \text{PDF}(\mathbf{d})\text{PDF}(\boldsymbol{\alpha}) \\ &= \frac{1}{\sqrt{(2\pi)^n |\mathbf{V}_d|}} \exp(-(\mathbf{d} - \langle \mathbf{d} \rangle)^T \mathbf{V}_d^{-1} (\mathbf{d} - \langle \mathbf{d} \rangle)) \\ &\quad \times \frac{1}{\sqrt{(2\pi)^m |\mathbf{V}_\alpha|}} \exp(-(\boldsymbol{\alpha} - \langle \boldsymbol{\alpha} \rangle)^T \mathbf{V}_\alpha^{-1} (\boldsymbol{\alpha} - \langle \boldsymbol{\alpha} \rangle)) \end{aligned} \quad (5.1)$$

where  $n$  is the number of measurements and  $m$  is the number of model parameters. Combining the exponentials gives

$$\begin{aligned} \text{PDF}(\mathbf{d}, \boldsymbol{\alpha}) &= \\ &= \frac{1}{\sqrt{(2\pi)^{n+m} |\mathbf{V}_d| |\mathbf{V}_\alpha|}} \exp(-(\mathbf{d} - \langle \mathbf{d} \rangle)^T \mathbf{V}_d^{-1} (\mathbf{d} - \langle \mathbf{d} \rangle) - (\boldsymbol{\alpha} - \langle \boldsymbol{\alpha} \rangle)^T \mathbf{V}_\alpha^{-1} (\boldsymbol{\alpha} - \langle \boldsymbol{\alpha} \rangle)) \end{aligned} \quad (5.2)$$

We now introduce the constraint associated with the model. If the model is correct, then we expect that the model, when evaluated at the true value for  $\boldsymbol{\alpha}$ , will give predictions that agree with the expected value (or equivalently the mode) for the measurements  $\mathbf{d}$ . In

other words, the model  $\mathbf{m}$  gives

$$\langle \mathbf{d} \rangle = \mathbf{m}(\boldsymbol{\alpha}) \quad (5.3)$$

Substituting Eq. (5.3) into (5.2) gives

$$\text{PDF}(\mathbf{d}, \boldsymbol{\alpha}) = \frac{1}{4\pi^2 \sqrt{(2\pi)^{n+m} |\mathbf{V}_d| |\mathbf{V}_\alpha|}} \exp(-(\mathbf{d} - \mathbf{m}(\boldsymbol{\alpha}))^T \mathbf{V}_d^{-1} (\mathbf{d} - \mathbf{m}(\boldsymbol{\alpha})) - (\boldsymbol{\alpha} - \langle \boldsymbol{\alpha} \rangle)^T \mathbf{V}_\alpha^{-1} (\boldsymbol{\alpha} - \langle \boldsymbol{\alpha} \rangle)) \quad (5.4)$$

We wish to choose the  $\boldsymbol{\alpha}$  that maximizes the above PDF( $\mathbf{d}, \boldsymbol{\alpha}$ ). This is equivalent choosing the  $\boldsymbol{\alpha}$  that minimizes the following:

$$r^2 = (\mathbf{d} - \mathbf{m}(\boldsymbol{\alpha}))^T \mathbf{V}_d^{-1} (\mathbf{d} - \mathbf{m}(\boldsymbol{\alpha})) + (\boldsymbol{\alpha} - \langle \boldsymbol{\alpha} \rangle)^T \mathbf{V}_\alpha^{-1} (\boldsymbol{\alpha} - \langle \boldsymbol{\alpha} \rangle) \quad (5.5)$$

The known variables in Eq. (5.5) are the measurement vector  $\mathbf{d}$ , the expected vector of parameters  $\langle \boldsymbol{\alpha} \rangle$ , and the covariance matrices  $\mathbf{V}_d$  and  $\mathbf{V}_\alpha$ . The only unknown in Eq. (5.5) is the vector of model parameters  $\boldsymbol{\alpha}$  to be estimated. As discussed in Chapter 3, we use the sensitivity based approximation to the model given by (3.1) for  $\mathbf{m}(\boldsymbol{\alpha})$ . Standard optimization programs (such as those provided by IMSL, 1997, or Mathematica, 1996) can be used to find the  $\boldsymbol{\alpha}$  that minimizes Eq. (5.5). Here we used the Mathematica routine FindMinimum to find the parameters  $\boldsymbol{\alpha}$  that minimizes Eq. (5.5), which is equivalent to maximizing Eq. (5.4). The resulting parameter values are listed in Table 5.1. The  $r^2$  at our minimum was found to be

$$r^2 = 14.60 \quad (5.6)$$

**Table 5.1: The Most Likely Model Parameters for the Heat Conduction Data**

$\alpha_1$ (i.e., thermal conductivity, $k$ )	14.70 W/m-°C
$\alpha_2$ (i.e., volumetric head capacity, $C$ )	$3.885 \times 10^6$ J/m <sup>3</sup> -°C
$\alpha_3$ (i.e., contact conductance, $h$ )	1692. W/m <sup>2</sup> -°C

We would now like to know the probability of obtaining this  $r^2$  or a larger value (i.e., a smaller PDF value) for a valid model. For the case of the multinormal distributions considered here (i.e., Eq. (5.4)), the cumulative PDF for  $r^2$  is given by the

$\chi^2(k)$  distribution, where  $k$  is the number of degrees of freedom (Beck and Arnold, 1977). In our case, we have 10 measurements that correspond to 10 degrees of freedom. The probability that we could have an  $r^2 > 14.60$  is given by (see any statistical text book that lists probabilities for the  $\chi^2(k)$  distribution)

$$P(\chi^2(10) > 14.60) = 0.147 \quad (5.7)$$

Note that the probability of obtaining these results or worse (i.e., the significance) given that the model is valid, is 14.7%. Thus a correct model would give this large of a  $r^2$  for 14.7% of the realizations of the model validation exercise. Normally, we would not reject the model unless we obtain a smaller level of significance, say 5%, to give the benefit of the doubt to the model. Therefore, this data does not provide sufficient evidence to reject the model at the 95% confidence level (i.e., 95% confidence that we do not reject a valid model). Nor does it provide sufficient evidence to reject the model at the 90% confidence level (or level of significance = 10%).

### 5.3 Application to Shock Physics Application

We now demonstrate this approach using the shock wave physics application. As discussed in Chapter 3, Hills and Trucano (2001) used the Kolmogorov-Smirnov test to evaluate the normality of the measurement and model parameters uncertainty and did not find sufficient evidence to reject the normality of these distributions. We therefore use multi-normal distributions to model the uncertainty in the measurements and in the model parameters. A summary of the statistics is provided in Table 5.2 (see Eq. (3.2) and Table 3.5).

**Table 5.2: Statistics for the Shock Physics Application**

Parameters	Expected Values	Covariance Matrix	
		$\alpha_1$	$\alpha_2$
The model			
$\alpha_1$ (i.e. $C_s$ )	5344	166.4	-0.0663
$\alpha_2$ (i.e. $S_1$ )	1.305	-0.0663	3.50 E-5
The measurements			
$d_i, i=1,120$	$\langle d_i \rangle$ , unknown	83.7 <sup>2</sup> <b>I</b>	

Given the measurement vector of the 120 measurements provided in Table 3.4, and a response surface model for the CTH defined by Table 3.7, we find the  $\alpha$  that minimizes  $r^2$  using the IMSL routine bconf (IMSL, 1997). The degrees of freedom for this example is the number of measurements and is  $k=120$ . The results of the optimization process are shown in Table 5.3. We also show the  $r^2$  value obtained and the cumulative probability of obtaining a larger  $r^2$  for a valid model. Note that the probability of obtaining a larger  $r^2$  is 25.9%, which is the significance of this result. Thus, if we were to repeat this exercise many times, we would expect that a valid model would give worse results (larger  $r^2$ ) approximately 25.9% of the time. Generally, one does not reject a model as valid unless there is a much smaller probability (say 5%) that a valid model could produce such results. So based on this test, we do not reject the model as valid. The measurements are statically consistent with the model.

**Table 5.3: The Most Likely Model Parameters for the Shock Physics Application**

$\alpha_1$ (i.e. $C_s$ )	5345.9 m/s
$\alpha_2$ (i.e. $S_I$ )	1.2978
minimum $r^2$	129.58
$P(\chi^2(120) > 129.58)$	25.9%

#### **5.4 Non-Normally Distributed Parameters and Measurements**

The methods used in the previous sections took advantage of our knowledge that the measurement and parameter uncertainty was normally distributed. Specifically, we used the  $\chi^2(k)$  statistic to evaluate the probability that the valid model would have differences between prediction and observations as large or larger than those observed. This distribution is based on our underlying multinormal distributions for the measurement and model parameters uncertainty. How would we apply this procedure if our underlying distributions were not normal?

One of the advantages of the maximum likelihood approach is it can easily be applied to nonlinear models with non-normally distributed measurements and parameters. To demonstrate this, we apply the method to the shock physics problem considered above. Specifically, we use the response surface approximation for the dependence of the shock speed on the particle velocity and the two EOS model parameters. To illustrate the application of various types of probability distributions, we assume that the uncertainty in the  $C_s$  model parameter is normally distributed, the uncertainty in the  $S_I$  model parameter is triangularly distributed, and the uncertainty in the measurements are well represented by a Beta distribution, as introduced in Chapter 3. The normal distribution requires two

parameters to define it – the mean and standard deviation. The triangular distribution is also based on two parameters, a lower and an upper bound of the distribution. In contrast, the Beta distribution requires 4 parameters – the lower and upper bounds, and two additional parameters defining the shape of the distributions. Because of the extra parameters of the Beta distribution, it can be used to approximate the distributions for a wide variety of applications for which a lower and upper bound exist. A special case of the Beta distribution is the uniform distribution.

Equations (3.4), (3.8), and (3.9) define the functional relationship for the three distributions. Table 3.6 lists the distributional parameter used here. This table is reproduced below as Table 5.4.

**Table 5.4: Distribution Parameters for Alternate Probability Models**

Variable	Distribution	Parameter	Value
$\alpha_1 (C_s)$	Normal	$\langle \alpha_1 \rangle$	5344 m/s
		$\sigma$	12.90 m/s
$\alpha_2 (S_1)$	Triangular	$\alpha_{2-lb}$	1.287
		$\alpha_{2-ub}$	1.323
$\mathbf{d}$	Beta	$\mathbf{d}_{ub}-\mathbf{d}_{lb}$	502.2, m/s
		$b_1$	3.0
		$b_2$	2.0

The joint probability density for the two model parameters and the 120 measurements is given by

$$\begin{aligned} \text{PDF}(\boldsymbol{\alpha}, \mathbf{d}, \mathbf{p}) = & \text{PDF}_{\text{normal}}(\langle \alpha_j \rangle, \sigma, \alpha_1) \text{PDF}_{\text{triangular}}(\alpha_{2-lb}, \alpha_{2-ub}, \alpha_2) \\ & \times \text{PDF}_{\text{beta}}(d_{1-lb}, d_{1-ub}, b_1, b_2, d_1) \dots \text{PDF}_{\text{beta}}(d_{120-lb}, d_{120-ub}, b_1, b_2, d_{120}) \end{aligned} \quad (5.8)$$

Where  $\boldsymbol{\alpha}$  and  $\mathbf{d}$  are the vectors of 2 model parameters and 120 experimental measurements and  $\mathbf{p}$  is the vector of the parameters defining the probability distributions (Column 3 in Table 5.4). Rather than evaluate (5.8) at the values for the parameters and measurements, we evaluate the joint PDF using normalized PDFs. This improves the efficiency of the algorithm somewhat during the last step of evaluating cumulative probabilities. Using (3.4b), (3.8b), and (3.9b) to normalize the parameters, (5.8) can be written as

$$\text{PDF}(\boldsymbol{\alpha}, \mathbf{d}, \mathbf{p}) = \text{PDF}_{\text{normal}}(x_n) \text{PDF}_{\text{triangular}}(x_t) \times \text{PDF}_{\text{beta}}(b_1, b_2, x_{b-1}) \dots \text{PDF}_{\text{beta}}(b_1, b_2, x_{b-120}) \quad (5.9)$$

We assume that our model, when evaluated at the true model parameters, will give us the mode for the measurements.

$$\mathbf{d}_{\text{mode}} = \mathbf{m}(\boldsymbol{\alpha}) \quad (5.10)$$

We could also assume that the model, when evaluated at the true values for the parameters, gives us the expected value for the measurements. For the previous examples, both of these approaches were equivalent since the normal distribution is symmetric. However, for the case of a non-symmetric Beta distribution (i.e.,  $b_1 \neq b_2$ ), these approaches give somewhat different results since the expected value and the mode occur at different locations in the distribution. The expected value (mean) and the mode for the Beta distribution occurs at

$$\langle x \rangle = \frac{b_1}{b_1 + b_2} \quad (5.11)$$

$$x_{\text{mode}} = \frac{b_1 - 1}{b_1 + b_2 - 2} \quad (5.12)$$

We need to define the upper and lower bounds of the Beta distribution for each measurement. These bounds will be a function of the estimated value for the vector  $\mathbf{d}_{\text{mode}}$ . For purposes of illustration, we choose the width of the Beta distribution to be six times the standard deviation estimated for the measurement uncertainty (see Table 5.4). Given an estimated value for  $\mathbf{d}_{\text{mode}}$ , our upper and lower bounds are given by

$$\mathbf{d}_{\text{lb}} = \mathbf{d}_{\text{mode}} - 3 \cdot 83.7 x_{\text{mode}} \quad (5.13)$$

$$\mathbf{d}_{\text{ub}} = \mathbf{d}_{\text{mode}} + 3 \cdot 83.7 (1 - x_{\text{mode}}) \quad (5.14)$$

While we know the width of the Beta distribution, we are using the maximum likelihood procedure to estimate the location of the distribution.

We are now ready to apply the maximum likelihood technique. To find the modes of the measurements and model parameters that are most likely, we use the gradient based minimization routine IMSL routine bconf (IMSL, 1997) to search over the model parameter space as follows:

A function evaluation routine must be provided that evaluates the objective function given a guess for the parameter vector  $\alpha$ . Our routine performed the following

1. Evaluate the corresponding most likely measurements using the response surface approximation to Eq. (5.10)
2. Evaluate the corresponding lower and upper bounds for the measurement distributions using the parameters in Table 5.4 and Eqs. (5.12) through (5.14).
3. Using the results of items 1 and 2 and the parameters listed in Table 5.4, evaluate the resulting joint probability density from Eq. (5.9). Return the negative of the joint probability density to the calling routine bconf. The negative was returned since we wish to maximize rather than minimize the probability density.
4. The previous 3 steps are repeated for different iterations on the parameter values  $\alpha$  until the minimum of  $(-\text{PDF}(\alpha, \mathbf{d}, \mathbf{p}))$  is found.

Table 5.5 lists the resulting parameter vector that maximizes the joint probability density. The corresponding probability density is also listed. Note that these parameters are somewhat different than those shown in Table 5.3. We expect this to be true since different probability distributions have been assumed for the model parameters and the experimental measurements. Given these estimates for the model parameters, we can use (5.9) to obtain the corresponding estimate of the modes for the measurements. We now need to evaluate the probability of obtaining these model parameters and modes, given that the model is valid.

**Table 5.5: Maximum Likelihood Parameters**

Parameter	Estimated Value
$\alpha_1 (C_s)$	5342 m/s
$\alpha_2 (S_1)$	1.304
$\max(\text{PDF}(\alpha, \mathbf{d}, \mathbf{p}))$	$3.270 \times 10^{17}$

The approach used here, and introduced in Chapter 4, is to evaluate the cumulative probability outside the equal probability density surface that passes through our estimated parameters/measurements using a Monte Carlo technique.

If our model is valid, our uncertainty will be due only to uncertainty in the model parameters and the experimental measurements. The PDF for our uncertainty is defined

by (5.9). We use the estimates for the parameters (Table 5.5) in Eq. (5.9) to obtain the corresponding joint probability density. We would like to evaluate the cumulative probability of obtaining this probability density, or smaller, to evaluate the significance of the estimated model parameters and the observed measurements given that the model is valid. The Monte Carlo procedure discussed in Chapter 4 is used and does not require any additional model evaluations. Specifically, we do the following:

1. Generate random values for the normalized model parameters and the normalized measurements and evaluate the joint PDF using (5.9).
2. Count the percentage of points that the resulting  $\text{PDF} < \max(\text{PDF}(\boldsymbol{\alpha}, \mathbf{d}, \mathbf{p}))$  (see Table 5.5). This represents the cumulative probability or significance that a model validation experiment with a valid model would have values for the measurements and parameters with less probability density than that observed here.

Here we used 50,000 sets of random numbers (each set is comprised of a unit normal random number, a triangular distribution random, and 120 Beta distribution random numbers) to generate the cumulative probability. The results were 49863 of these sets of random numbers had a joint PDF that was less than that given in Table 5.5. Thus we can say that the probability of a good model having a PDF less than that observed is 99.7%. This is quite large, indicating that there is no evidence to reject the model at 99.7% significance. Generally, we don't reject the model until we are at significantly small level of significance, such as 5%, because we want the probability of rejecting a good model to be very small. Note that the 99.7% level obtained here, is significantly larger than that obtained using normal distributions. This is because the alternative distributions used here have more cumulative probability outside the constant PDF that corresponded to the maximum likelihood model prediction than was the case for the normal distributions.

## 6.0 Equivalence to Previous Metric

In previous work (Hills and Trucano, 2001), the metric used to measure model validity in the presence of normally distributed predictions and experimental measurements was

$$r^2 = (\mathbf{d} - \mathbf{m}(\langle \alpha \rangle))^T (\mathbf{V}_d + \mathbf{V}_m)^{-1} (\mathbf{d} - \mathbf{m}(\langle \alpha \rangle)) \quad (6.1)$$

This expression was derived by looking at the uncertainty in the differences between model predictions and experimental observations.  $\mathbf{V}_m$  is the covariance matrix for the model predictions. Hills and Trucano found that  $r^2=129.6$  by this metric for the data set used here. In contrast, here we minimized (see Eq. (5.5))

$$r^2 = (\mathbf{d} - \mathbf{m}(\alpha))^T \mathbf{V}_d^{-1} (\mathbf{d} - \mathbf{m}(\alpha)) + (\alpha - \langle \alpha \rangle)^T \mathbf{V}_\alpha^{-1} (\alpha - \langle \alpha \rangle) \quad (6.2)$$

Note that the minimum  $r^2$  obtained for the maximum likelihood estimate (Table 5.3) obtained here was 129.58. This agrees with the  $r^2=129.6$  value obtained by Hills and Trucano using Eq. (6.1). This suggests that in some sense these metrics are related for this case.

Hills and Trucano (2001) used a sensitivity analysis to approximately relate changes in the model predictions to changes in model parameters:

$$\mathbf{m}(\alpha) \approx \mathbf{m}(\langle \alpha \rangle) + \mathbf{X}(\alpha - \langle \alpha \rangle) \quad (6.3)$$

where the sensitivity matrix is given by

$$\mathbf{X} = \nabla_\alpha \mathbf{m}(\langle \alpha \rangle) \quad (6.4)$$

This sensitivity matrix was used to estimate the covariance matrix for the model predictions

$$\mathbf{V}_m = \mathbf{X} \mathbf{V}_\alpha \mathbf{X}^T \quad (6.5)$$

Using Eq. (6.5) in (6.1) gives

$$r^2 = (\mathbf{d} - \mathbf{m}(\langle \alpha \rangle))^T (\mathbf{V}_d + \mathbf{X} \mathbf{V}_\alpha \mathbf{X}^T)^{-1} (\mathbf{d} - \mathbf{m}(\langle \alpha \rangle)) \quad (6.6)$$

We see that this metric is not of the same form as Eq. (6.2). However, if we evaluate Eq. (6.2) at those values for  $\langle \mathbf{d} \rangle$  and  $\alpha$  that minimize Eq. (6.2), and we use the sensitivity

analysis approximation, Eq. (6.3), for the model, then we anticipate that the two metrics may be equivalent. We now show that this is true.

We begin by using the sensitivity analysis approximation for the model that was used in previous work. Using (6.3) in (6.2) gives

$$r^2 = (\mathbf{d} - \mathbf{m}(\langle \alpha \rangle) - \mathbf{X}(\alpha - \langle \alpha \rangle))^T \mathbf{V}_d^{-1} (\mathbf{d} - \mathbf{m}(\langle \alpha \rangle) - \mathbf{X}(\alpha - \langle \alpha \rangle)) + (\alpha - \langle \alpha \rangle)^T \mathbf{V}_\alpha^{-1} (\alpha - \langle \alpha \rangle) \quad (6.7)$$

or

$$r^2 = (\alpha - \langle \alpha \rangle)^T \mathbf{V}_\alpha^{-1} (\alpha - \langle \alpha \rangle) + (\mathbf{d} - \mathbf{m}(\langle \alpha \rangle))^T \mathbf{V}_d^{-1} (\mathbf{d} - \mathbf{m}(\langle \alpha \rangle)) - 2(\alpha - \langle \alpha \rangle)^T \mathbf{X}^T \mathbf{V}_d^{-1} (\mathbf{d} - \mathbf{m}(\langle \alpha \rangle)) \quad (6.8)$$

We now determine values of  $\alpha$  that minimize Eq. (6.8) by taking the gradient with respect to  $\alpha$  and set the result to zero.

$$\nabla_\alpha r^2 = 2(\mathbf{V}_\alpha^{-1} + \mathbf{X}^T \mathbf{V}_d^{-1} \mathbf{X})(\alpha - \langle \alpha \rangle) - 2\mathbf{X}^T \mathbf{V}_d^{-1} (\mathbf{d} - \mathbf{m}(\langle \alpha \rangle)) = 0 \quad (6.9)$$

or

$$(\mathbf{V}_\alpha^{-1} + \mathbf{X}^T \mathbf{V}_d^{-1} \mathbf{X})(\alpha - \langle \alpha \rangle) = \mathbf{X}^T \mathbf{V}_d^{-1} (\mathbf{d} - \mathbf{m}(\langle \alpha \rangle)) \quad (6.10)$$

Using (6.10) in (6.8) gives the minimum value for  $r^2$ :

$$r_{\min}^2 = (\alpha - \langle \alpha \rangle)^T (\mathbf{V}_\alpha^{-1} + \mathbf{X}^T \mathbf{V}_d^{-1} \mathbf{X})(\alpha - \langle \alpha \rangle) + (\mathbf{d} - \mathbf{m}(\langle \alpha \rangle))^T \mathbf{V}_d^{-1} (\mathbf{d} - \mathbf{m}(\langle \alpha \rangle)) - 2(\alpha - \langle \alpha \rangle)^T \mathbf{X}^T \mathbf{V}_d^{-1} (\mathbf{d} - \mathbf{m}(\langle \alpha \rangle)) \quad (6.11)$$

or

$$r_{\min}^2 = (\mathbf{d} - \mathbf{m}(\langle \alpha \rangle))^T \mathbf{V}_d^{-1} (\mathbf{d} - \mathbf{m}(\langle \alpha \rangle)) + (\alpha - \langle \alpha \rangle)^T (\mathbf{V}_\alpha^{-1} + \mathbf{X}^T \mathbf{V}_d^{-1} \mathbf{X})(\alpha - \langle \alpha \rangle) - 2(\alpha - \langle \alpha \rangle)^T (\mathbf{V}_\alpha^{-1} + \mathbf{X}^T \mathbf{V}_d^{-1} \mathbf{X})(\alpha - \langle \alpha \rangle) \quad (6.12)$$

or

$$r_{\min}^2 = (\mathbf{d} - \mathbf{m}(\langle \alpha \rangle))^T \mathbf{V}_d^{-1} (\mathbf{d} - \mathbf{m}(\langle \alpha \rangle)) - (\alpha - \langle \alpha \rangle)^T (\mathbf{V}_\alpha^{-1} + \mathbf{X}^T \mathbf{V}_d^{-1} \mathbf{X})(\alpha - \langle \alpha \rangle) \quad (6.13)$$

Eq. (6.10) gives

$$(\alpha - \langle \alpha \rangle) = (\mathbf{V}_\alpha^{-1} + \mathbf{X}^T \mathbf{V}_d^{-1} \mathbf{X})^{-1} \mathbf{X}^T \mathbf{V}_d^{-1} (\mathbf{d} - \mathbf{m}(\langle \alpha \rangle)) \quad (6.14)$$

Using Eq. (6.14) in (6.13) leads to

$$\begin{aligned} r_{\min}^2 &= -(\mathbf{d} - \mathbf{m}(\langle \alpha \rangle))^T \mathbf{V}_d^{-1} \mathbf{X} (\mathbf{V}_\alpha^{-1} + \mathbf{X}^T \mathbf{V}_d^{-1} \mathbf{X})^{-1} \mathbf{X}^T \mathbf{V}_d^{-1} (\mathbf{d} - \mathbf{m}(\langle \alpha \rangle)) \\ &\quad + (\mathbf{d} - \mathbf{m}(\langle \alpha \rangle))^T \mathbf{V}_d^{-1} (\mathbf{d} - \mathbf{m}(\langle \alpha \rangle)) \end{aligned} \quad (6.15)$$

or

$$r_{\min}^2 = (\mathbf{d} - \mathbf{m}(\langle \alpha \rangle))^T \left( \mathbf{V}_d^{-1} - \mathbf{V}_d^{-1} \mathbf{X} (\mathbf{V}_\alpha^{-1} + \mathbf{X}^T \mathbf{V}_d^{-1} \mathbf{X})^{-1} \mathbf{X}^T \mathbf{V}_d^{-1} \right) (\mathbf{d} - \mathbf{m}(\langle \alpha \rangle)) \quad (6.16)$$

Note the following:

$$\begin{aligned} &(\mathbf{V}_d + \mathbf{X} \mathbf{V}_\alpha \mathbf{X}^T) \left( \mathbf{V}_d^{-1} - \mathbf{V}_d^{-1} \mathbf{X} (\mathbf{V}_\alpha^{-1} + \mathbf{X}^T \mathbf{V}_d^{-1} \mathbf{X})^{-1} \mathbf{X}^T \mathbf{V}_d^{-1} \right) \\ &= \mathbf{I} + \mathbf{X} \mathbf{V}_\alpha \mathbf{X}^T \mathbf{V}_d^{-1} - (\mathbf{V}_d + \mathbf{X} \mathbf{V}_\alpha \mathbf{X}^T) \mathbf{V}_d^{-1} \mathbf{X} (\mathbf{V}_\alpha^{-1} + \mathbf{X}^T \mathbf{V}_d^{-1} \mathbf{X})^{-1} \mathbf{X}^T \mathbf{V}_d^{-1} \\ &= \mathbf{I} + \mathbf{X} \mathbf{V}_\alpha \mathbf{X}^T \mathbf{V}_d^{-1} - (\mathbf{X} + \mathbf{X} \mathbf{V}_\alpha \mathbf{X}^T \mathbf{V}_d^{-1} \mathbf{X}) (\mathbf{V}_\alpha^{-1} + \mathbf{X}^T \mathbf{V}_d^{-1} \mathbf{X})^{-1} \mathbf{X}^T \mathbf{V}_d^{-1} \\ &= \mathbf{I} + \mathbf{X} \mathbf{V}_\alpha \mathbf{X}^T \mathbf{V}_d^{-1} - \mathbf{X} \mathbf{V}_\alpha (\mathbf{V}_\alpha^{-1} + \mathbf{X}^T \mathbf{V}_d^{-1} \mathbf{X}) (\mathbf{V}_\alpha^{-1} + \mathbf{X}^T \mathbf{V}_d^{-1} \mathbf{X})^{-1} \mathbf{X}^T \mathbf{V}_d^{-1} \\ &= \mathbf{I} \end{aligned} \quad (6.17)$$

Also note that (6.16) can be written

$$\begin{aligned} r_{\min}^2 &= (\mathbf{d} - \mathbf{m}(\langle \alpha \rangle))^T (\mathbf{V}_d + \mathbf{X}^T \mathbf{V}_\alpha \mathbf{X})^{-1} (\mathbf{V}_d + \mathbf{X}^T \mathbf{V}_\alpha \mathbf{X}) \\ &\quad \left( \mathbf{V}_d^{-1} - \mathbf{V}_d^{-1} \mathbf{X} (\mathbf{V}_\alpha^{-1} + \mathbf{X}^T \mathbf{V}_d^{-1} \mathbf{X})^{-1} \mathbf{X}^T \mathbf{V}_d^{-1} \right) (\mathbf{d} - \mathbf{m}(\langle \alpha \rangle)) \end{aligned} \quad (6.18)$$

Using Eq. (6.17) in (6.18) gives

$$r_{\min}^2 = (\mathbf{d} - \mathbf{m}(\langle \alpha \rangle))^T (\mathbf{V}_d + \mathbf{X}^T \mathbf{V}_\alpha \mathbf{X})^{-1} (\mathbf{d} - \mathbf{m}(\langle \alpha \rangle)) \quad (6.19)$$

Note that Eq. (6.19) is the same form as Eq. (6.6). The metrics used for the example problems in the previous work (Hills and Trucano, 1999, 2001) are thus equivalent to the metric based on maximum likelihood for the conditions considered.

To be more specific, we have shown that these two approaches are equivalent if

1. The uncertainty in the model parameters and the measurements can be well

modeled by multinormal distributions, and

2. The change in the model predictions due to changes in the model parameters can be modeled by the first two terms (i.e., a first order uncertainty analysis) in the Taylor series expansion.

Both of these assumptions were the assumptions used for the demonstration problems in the previous work. It should be noted however, that while both methods give the same results for the above assumptions, the intent of each method is different.

The intent of the metric given by Eq. (6.1) is to evaluate the probability that the observed differences between the expected value of the model predictions and the measurements are significant relative to the uncertainty in these differences. The intent of the maximum likelihood method, as used here, is to first calibrate the model using prior knowledge of the measurement and the parameter distributions, then look at the significance of obtaining the corresponding calibrated parameter values and observed measurements. If this probability is small, we question the validity of the model. This difference is significant, especially if the expected value of the model predictions is different than the value of the model predictions using the expected value of the model parameters. We expect this to be the case for models that are highly nonlinear over the range of model parameters corresponding to their uncertainty for the validation experiments.

If we are interested in characterizing the uncertainty in the model predictions, then we should propagate the model parameter uncertainty through the model. This is easy to do for the present case, but generally more difficult for highly nonlinear cases, or for cases where the probability distributions of the model parameters are more complex. However, if we are interested in model validation, then it can be argued that we are really interested in the probability of the specific model validation exercise outcome. This would suggest that we look at the probability of the calibrated model parameters and the probability of the measurements, given a valid model.

The advantage of the maximum likelihood approach is that we can use optimization methods to search for the maximum likely measurement-mode/model parameter set, given that the model is valid. We can then evaluate the probability that a valid model would give this set of values. This requires that we search through the uncertainty spaces for the model parameters, rather than the space of differences. This is generally much easier since we do not need to propagate the model parameter uncertainty through the model, we must only use the model predictions themselves. In addition, we only have to characterize the probability of obtaining the scalar quantity  $r^2$  rather than define the full  $n$ -dimensional validation space associated with the differences. The computation savings are significant.

## 7.0 Univariate Confidence Intervals

### 7.1 Introduction

We now look on the dangers of using univariate confidence intervals to judge model validity with multivariate data. Figure 7.1 shows the time trace of nine of the ten average temperatures and the corresponding model predictions for the thermal contact resistance data listed in Table 3.2. Also shown are the 95% univariate confidence intervals on the measurements and the model predictions. The confidence intervals on the measurements are based on the standard deviations given in Table 3.2. The confidence intervals on the model predictions were obtained using the diagonal terms of the predicted covariance matrix (see Eq. 6.5), which in turn, was obtained using the sensitivity analysis discussed in an earlier section. Procedures to obtain these limits are also discussed in Hills and Trucano (1999, 2001).

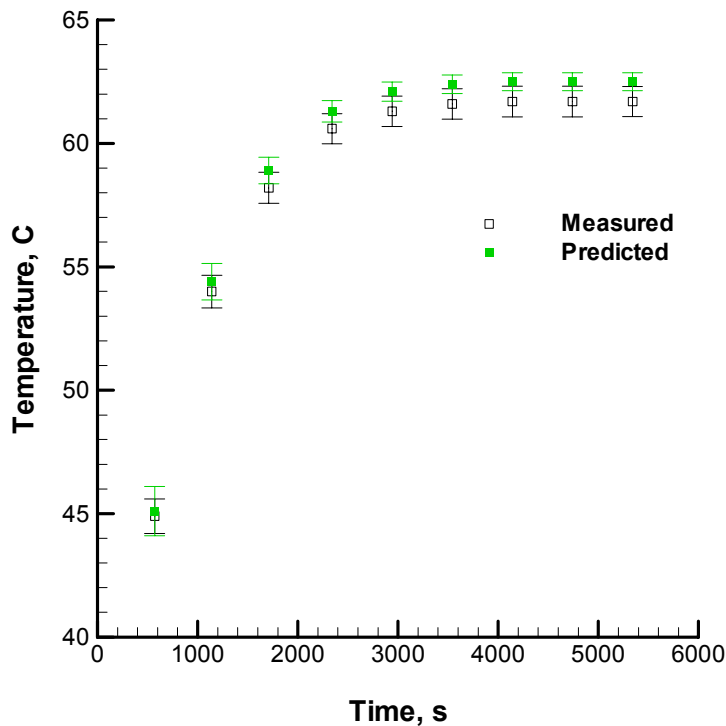


**Figure 7.1:** Experimental and Predicted Data. Time zero data are not shown. Confidence intervals are based on normal distributions at 95% confidence and univariate statistics.

Note that the confidence intervals of the measurements and model predictions overlap at all times. What does this mean in terms of model validity? To better address this issue, first combine the intervals of the measurements and model predictions into single confidence intervals. Since we are assuming that the measurement and the predictions are independent, the variance for the difference between the predictions and the measurements is equal to the sum of variances (i.e., square of the standard deviations) of the prediction and the measurements (Beck and Arnold, 1977).

$$\sigma_{\text{total}}^2 = \sigma_{\text{meas}}^2 + \sigma_{\text{pred}}^2 \quad (7.1)$$

The confidence intervals corresponding to this total is shown in Figure 7.2. We could also show these as intervals about the measurements. Since the intervals are symmetric, both approaches will give the same results. Note that the early time measurements lie within the confidence intervals, but the late time measurements are slightly outside the intervals. Does this mean the model is valid for this application of the validation experiment? At first glance, one might say no. But the issue of validity is complicated by correlation in the data. To investigate this further, we look at validation metrics in more detail for this set of data.

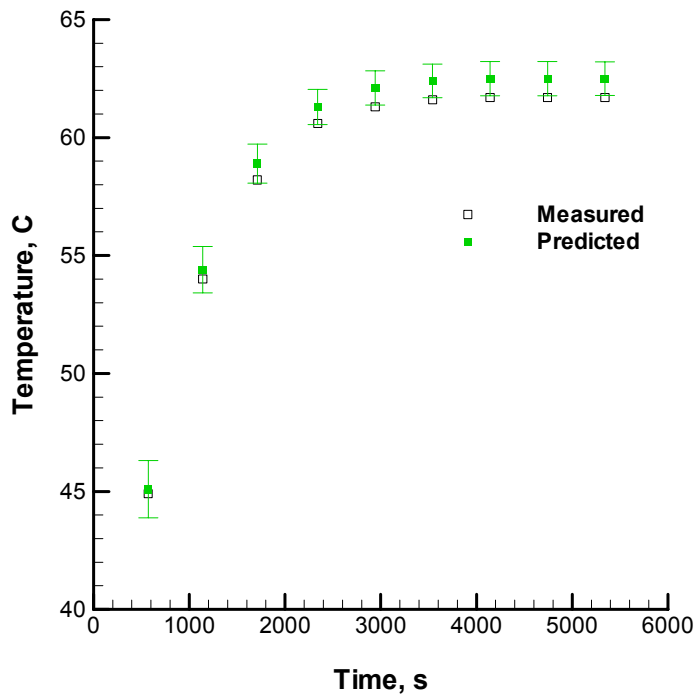


**Figure 7.2: Experimental and Predicted Data.** Time zero data are not shown. Combined confidence intervals are based on normal distributions at 95% confidence and univariate statistics.

For this discussion, we use the metric defined by Hills and Trucano (2001) rather than the maximum likelihood based metric developed in this report. We use this metric here (i.e., Eq. (6.1)) because it is more intuitive from a graphical point of view. As was shown in the previous chapter, this metric and the maximum likelihood metric give the same results for this particular analysis.

## 7.2 Two Measurement Times

To investigate the meaning of the results illustrated in Figure 7.2, we begin by looking at the joint probability of two measurements lying inside or outside the confidence intervals. Surfaces of constant joint probability density function (PDF) for a vector of normally distributed random variables are given by constant values of  $r^2$  where (Hills and Trucano, 2001)

$$r^2 = \mathbf{x}^T \mathbf{V}^{-1} \mathbf{x} \quad (7.2)$$

$\mathbf{x}$  is a vector of normally distributed random variables and  $\mathbf{V}$  is the corresponding covariance matrix for the vector. Here (see Eq. (6.1)) we take  $\mathbf{x}$  to be the vector of differences between model predictions and experimental observations.  $\mathbf{V}$  is the covariance matrix for these differences. Surfaces of constant  $r^2$  correspond to  $n$ -dimensional ellipses where  $n$  is the number of measurements. The cumulative probability within some constant  $r^2$  ellipse is given by the  $r^2 = \chi^2(k)$  distribution for  $k$  degrees of freedom (Beck and Arnold, 1977).

For the purposes of example, we take the third and last measurement times of Figure 7.2 as our two measurements (the fourth and last measurements of Table 3.2). This provides a measurement in the transient phase as well as in the near steady-state phase of the experiment. Later we will extend this analysis to all 10 of the measurements listed in Table 3.2. The vector of differences between the predictions and the measurements for these two times is

$$\mathbf{d} = \begin{bmatrix} 0.63 \\ 0.80 \end{bmatrix} \quad (7.3)$$

The diagonal of the covariance matrix for these two average measurements is given by the squares of the standard deviations listed in Table 3.2. Since we assumed the measurements are independent, the off diagonal elements are zero.

$$\mathbf{V}_{\text{meas}} = \begin{bmatrix} 0.1034 & 0 \\ 0 & 0.09803 \end{bmatrix} \quad (7.4)$$

Eq. (6.5) and the sensitivity coefficient listed in Table 3.2 are used to estimate the covariance matrix of the model predictions for the two measurement times of interest. This results in

$$\mathbf{V}_{\text{pred}} = \begin{bmatrix} 0.07489 & 0.04526 \\ 0.04526 & 0.03512 \end{bmatrix} \quad (7.5)$$

Note that the prediction matrix is not diagonal indicating that these two predictions are correlated. The sum of these matrices gives the correlation matrix for the differences between the predictions and observations (see Hills and Trucano, 2001).

$$\mathbf{V} = \mathbf{V}_{\text{meas}} + \mathbf{V}_{\text{pred}} = \begin{bmatrix} 0.17826 & 0.04526 \\ 0.04526 & 0.13316 \end{bmatrix} \quad (7.6)$$

We are now ready to define the constant PDF curves. The degrees of freedom is equal to the number of measurements (i.e.,  $k=2$ ). The  $r^2$  for a cumulative probability of 95% is

$$r_{0.95}^2 = \chi^2(k) = \chi^2(2) = 5.991 \quad (7.7)$$

These values are tabulated in most introductory statistics books or can be evaluated using common mathematical software packages (here we use Mathematica; see Wolfram, 1999). The equation describing this elliptical curve is thus (see Eq. (7.2))

$$\mathbf{x}^T \mathbf{V}^{-1} \mathbf{x} = 5.991 \quad (7.8)$$

The  $r^2$  for the differences between the predictions and measurements is

$$r^2 = 5.580 = \mathbf{d}^T \mathbf{V}^{-1} \mathbf{d} \quad (7.9)$$

Since 5.580 is less than 5.991, our difference lies within the 95% elliptical surface. We can thus say that we do not have sufficient evidence, at the 95% confidence level, that the model is not valid. So even though one of these two measurements lies outside the confidence intervals shown in Figure 7.2, we do not have sufficient evidence to reject the model as valid.

To illustrate the common assumption of independent differences, we ignore the off-diagonal terms in  $\mathbf{V}$  by setting them to zero (i.e., we are ignoring the correlation between the differences).

$$\mathbf{V} = \mathbf{V}_{\text{meas}} + \mathbf{V}_{\text{pred}} = \begin{bmatrix} 0.17826 & 0 \\ 0 & 0.13316 \end{bmatrix} \quad (7.10)$$

The  $r^2$  of our differences for this case is

$$r^2 = 7.03 = \mathbf{d}^T \mathbf{V}_{\text{ind}}^{-1} \mathbf{d} \quad (7.11)$$

Note that 7.03 is smaller than 5.991, indicating that the differences lies outside the 95% region. In this case, we do reject the model with 95% confidence. This is in contrast to the previous case when the correlation in the differences was properly accounted for.

Why do we obtain different results for the  $r^2$  when we assume that the measurements are independent? We can illustrate this by plotting the ellipses corresponding to dependent and independent cases. These are shown as the inclined and horizontal ellipses of Figure 7.3, respectively, along with the point corresponding to the differences  $\mathbf{d}$  at the two measurement times. As the figure illustrates, the differences between prediction and observation fell within 95% confidence region for the dependent case and outside it for the independent case. Since the 95% curves are oriented differently, we obtain different measures for  $r^2$  in either case. Clearly, we see that accounting for correlation is important, if such correlation in the differences is present.

A method that has been proposed (see Luis and McLaughlin, 1992) to test for model validity is to plot confidence intervals for the uncertainty of the differences for each difference, and evaluate the number of measurements that are outside these intervals. If 5% of these measurements lie outside the interval, Luis and McLaughlin suggests that we reject the model as valid. The 95% confidence intervals evaluated using Eq. (7.1) for the two measurements are shown as the rectangle in Figure 7.3. Note that the measurements lie within the intervals for the first measurement, but not for the second. This was also reflected by the third and last points of Figure 7.2. Thus, 50% of the two measurements are outside the interval, even through there is not sufficient evidence at the 95% confidence level to reject the model for the correlated case.

If the differences were independent, then the joint probability of lying inside the rectangle would be the products of the probabilities for the individual bounds. For this case, the cumulative probability is 90.2% ( $=0.95 \times 0.95$ ). This explains why the area of the rectangle is somewhat less than that of the horizontal ellipse. Even if one were to expand the individual bounds so that the cumulative probability within the rectangle is 95%, this would still not provide an appropriate test for model validity. For example, the measurement may still lie outside the interval for one measurement, but lie inside the interval for the other, and have a joint probability that lies within the 95% joint probability ellipse. What is important is the joint probability of the differences, not the number of differences that lie outside individual confidence intervals. This is why one

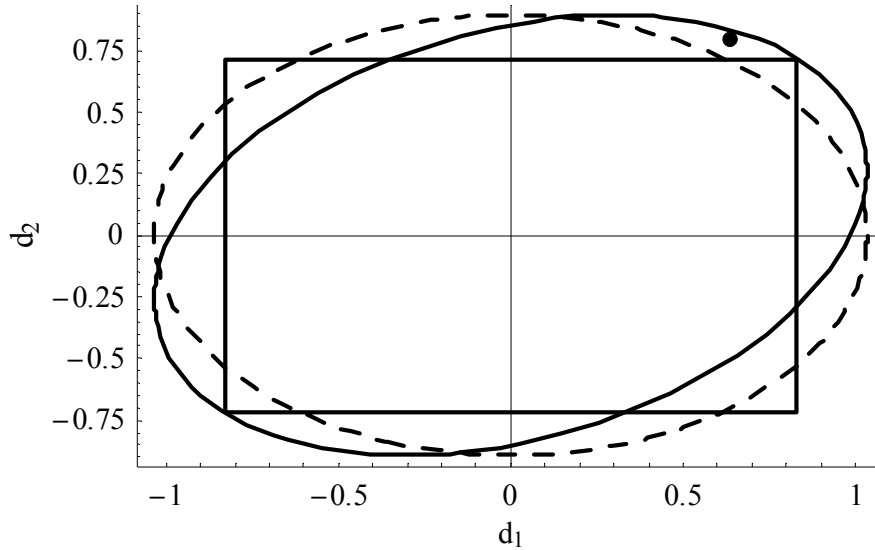


**Figure 7.3:** 95% Confidence Intervals on the Differences – 2 Measurements: Solid ellipse includes correlation, dashed ellipse ignores correlation, rectangle represents univariate confidence intervals, point is the difference.

must be cautious about using univariate confidence intervals to evaluate multivariate models.

### 7.3 More than 2 Measurement Times

How do we extend the above discussion to more than 2 measurements? The metrics defined above for  $r^2$  extend directly to the higher dimensional case. For the case of our 10 data pairs

$$r^2 = 14.60 = \mathbf{d}^T \mathbf{V}^{-1} \mathbf{d} \quad (7.12)$$

Note that we obtained the same result for  $r^2$  in Section 5.2 using the maximum likelihood approach. As the results of Chapter 6 show, we expect this equivalence for the analysis presented here. The degrees of freedom for 10 measurements is  $k=10$ . The critical value for  $r^2$  at 95% confidence is

$$r_{0.95}^2 = \chi^2(k) = \chi^2(10) = 18.31 \quad (7.13)$$

The vector of differences thus lies within this 95% confidence interval. How do we show this graphically for a 10 dimensional ellipse? Unfortunately, we can only plot two or three-dimensional representations of the 10-dimensional ellipses. Here we take the intersection of a 2-dimensional plane with the ellipse to reduce our graphical

representation to one we can picture. The plane we select contains the center of the ellipse and the measurement point to insure that our measurement point lies in the same plane as the intersection of the higher dimensional ellipse. A third point (or second vector) is needed to complete the definition of the plane. We choose that direction to represent a worst case in the sense that the measurement point is furthest from the center of the ellipse in this plane, as measured by our metric  $r^2$ . To represent our plane, we evaluate an orthogonal basis for it (i.e., two orthogonal vectors that lie in the plane). We take the first direction as the vector of differences to insure that the measurements lie in the selected plane:

$$\mathbf{v}_1 = \mathbf{d} \quad (7.14)$$

The second direction is the direction that maximizes the change in  $r^2$  at  $\mathbf{d}$ . This direction corresponds to the gradient of  $r^2$  at  $\mathbf{d}$  (i.e, the outward normal to the corresponding ellipse though  $\mathbf{d}$ ).

$$\mathbf{v}_2 = \nabla r^2 = 2\mathbf{V}\mathbf{d} \quad (7.15)$$

Using Gram-Schmidt orthogonalization to transform the above two vectors into an orthogonal basis and normalizing gives

$$\mathbf{v}'_2 = \mathbf{v}_2 - (\mathbf{v}_2 \cdot \mathbf{v}_1)\mathbf{v}_1 / (\mathbf{v}_1 \cdot \mathbf{v}_1) \quad (7.16)$$

$$\mathbf{u}_1 = \mathbf{v}_1 / \sqrt{\mathbf{v}_1 \cdot \mathbf{v}_1} \quad (7.17)$$

$$\mathbf{u}_2 = \mathbf{v}'_2 / \sqrt{\mathbf{v}'_2 \cdot \mathbf{v}'_2} \quad (7.18)$$

We can restrict  $\mathbf{x}$  (see Eq. (7.1)) to this plane by writing  $\mathbf{x}$  as a linear combination of this basis.

$$\mathbf{x} = [\mathbf{u}_1 \quad \mathbf{u}_2] \begin{bmatrix} y_1 \\ y_2 \end{bmatrix} = \mathbf{U}\mathbf{y} \quad (7.19)$$

where  $\mathbf{U}$  is a  $n \times 2$  orthonormal matrix. Substituting (7.19) into (7.1) gives

$$r^2 = \mathbf{y}^T \mathbf{U}^T \mathbf{V}^{-1} \mathbf{U} \mathbf{y} \quad (7.20)$$

The equation for our 95% confidence ellipse in the plane is thus

$$\mathbf{y}^T \mathbf{U}^T \mathbf{V}^{-1} \mathbf{U} \mathbf{y} = 18.31 \quad (7.21)$$

We also transform the vector of differences to represent it on the same basis or coordinate system.

$$\mathbf{d}' = \mathbf{U}\mathbf{d} \tag{7.22}$$

This ellipse (Eq. (7.21), along with the ellipse corresponding to the assumption of uncorrelated differences (i.e., the off-diagonal terms in  $\mathbf{V}$  are zero), the transformed difference of measurements, and the univariate confidence bounds are shown in Figure 7.4. Remember that we defined the plane in such a way so that the resulting difference appears to be as far from the center as possible, based on our measure of  $r^2$ . If we have picked any other plane, then the point may appear in the ellipse in Figure 7.4, when in fact it is outside the ellipse, suggesting that the model is better than it is actually is.

The result shown in Figure 7.4 illustrates that if we neglect correlation, the difference between prediction and measurements would appear outside the acceptance region. However, the acceptance region that accounts for correlation does include the measurement, and it also appears to include a larger area. This is due to the very significant correlation that occurs in the model predictions, which increases the level of uncertainty in the differences “along the direction of correlation”. The result is the elongated ellipse shown in Figure 7.4. As in the previous case, the use of univariate error

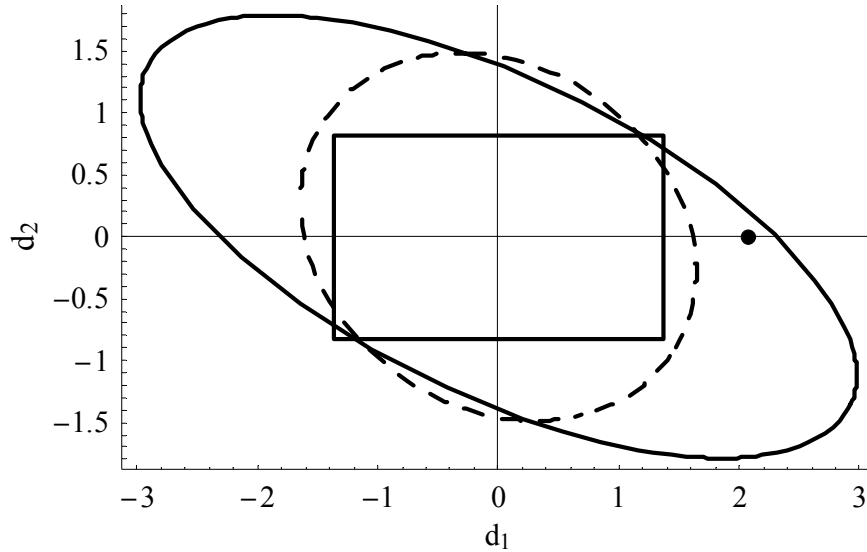


**Figure 7.4:** 95% Confidence Intervals on the Differences – 10 measurements: Solid ellipse includes correlation, dashed ellipse ignores correlation, rectangle represents univariate confidence intervals, point is the difference.

bounds (i.e., the rectangle in Figure 7.4) underestimates the region of acceptance for multivariate data. The use of univariate confidence intervals to evaluate multivariate data can clearly lead to very misleading results. In addition, we see that for this case, ignoring correlation will lead to the rejection of our thermal contact resistance model, when in fact, we do not have sufficient statistical evidence to do so.

#### **7.4 Correlation and the Maximum Likelihood Method**

The presentations given in the previous sections were based on the cumulative probability on the differences between the predictions and observations. The maximum likelihood method, which was presented earlier, evaluated the cumulative PDF on the parameters and measurements directly. In contrast to the approach used in this section, the maximum likelihood method does not require that we propagate uncertainty through the model. Hence, the model-induced correlations shown in the figures of this chapter do not directly enter into the maximum likelihood analysis. This model structure is accounted for during the optimization process used to estimate the true values of the model parameters and the mode of the measurements. The only correlation that one has to account for in the maximum likelihood method is the correlation between the model parameters themselves and between the measurements. However, as was shown in the previous chapter, the resulting metric values obtained are the same for the two methods for the analysis of the two applications considered here.

(Page left blank)

## **8.0 Discussion and Recommendations**

### ***8.1 The Approach***

The focus of the past 3 years work (Hills and Trucano, 1999, 2001, and the present report) represents a concentrated effort to understand issues involved with using statistical techniques to define metrics to test for model validity. While we provided an example to the contrary in the year 2 work, the primary focus of this work was on the development of methodology that can be applied to complex engineering systems for which we do not have sufficient experimental data to characterize the uncertainty directly from the observed differences between model predictions and the experimental observations. We do assume that we have more complete knowledge of the uncertainties in the model parameters and the experimental observations. These approaches require that we either propagate this model parameter uncertainty through the model (which requires multiple model evaluations) or that we use an optimization procedure (also requires multiple model evaluations) to find the most likely parameters, given prior knowledge of the measurement and parameter uncertainty. Thus the methodology introduced here replaces the need to run multiple, independent, validation experiments, with the need to run the model multiple times. It does not remove the need to perform validation experiments.

This approach is consistent with trends in computation and experimentation that are occurring at Sandia National Laboratories (SNL) and elsewhere. Experimental work is becoming more expensive, while computer modeling is becoming less time consuming and less expensive. Non-invasive software tools that drive computer models for engineered and physical systems to propagate uncertainty, or to perform optimization, are becoming more available to the computational community. Thus we feel that the present approach is justified as a complementary alternative to the more experimental intensive approach, which characterizes uncertainty between experimental observations and model predictions from the experimental data directly.

### ***8.2 Accomplishments Over the Past Three Years***

The five major accomplishments of the past 3 years work are the following:

1. This work emphasized issues associated with using rigorous statistical techniques to compare model predictions to experiment observations with an emphasis on multivariate data (years 1, 2, and 3).
2. We developed methodology to use the results of uncertainty propagation through predictive models, in association with the uncertainty in experimental

- measurements, to statistically measure consistency between measurements and predictions (year 2).
3. We introduced the principle of modifying these measures to reflect differences between the intended application of the model and the validation experiments (year 2).
  4. We introduced the idea of using maximum likelihood techniques to define an alternative (but related) measure of model validity (year 3).
  5. The metrics introduced in this work account for correlation in the differences between measurements and model predictions, due to model structure. We showed that neglecting such correlation or model structure, can lead to the rejection of a good model when the statistical evidence to do so is not sufficient, or can lead to the failure to reject a bad model when there is sufficient evidence to do so (year 3).

As we moved from item 1 to item 4, we also increased our ability to handle more complex models with less common probability distributions. While the metrics developed in year 2 are somewhat more intuitive, we feel that the less intuitive maximum likelihood metric developed in this report offers significant promise for complex probability distributions and highly nonlinear models.

### **8.3 Recommendations**

We feel that we have made significant progress in understanding the development of statistical metrics for validation of complex engineering models over the past years. Our primary focus during the next years should be on applying these metrics to applications of interest to SNL. As we do so, we expect a significant part of the work will be the identification of the appropriate probability models for the uncertainties. When we do not have sufficient information to do so, we may need to fall back on other approaches, such as the exploration of a subspace of probability models to see under what conditions (i.e., what probability models) our confidence in the models is questionable.

A secondary focus of future work should be on tying the anticipated application to the definition of the validation metrics. We introduced the idea of doing this during year 2. We used a sensitivity analysis to define the mappings between the anticipated application and the validation experiments. We suggest that the use of maximum likelihood techniques, rather than the propagation of uncertainty techniques used during year 2, may allow us to relax the need to depend on the locally linear assumption of the sensitivity analysis. This would allow us to consider more complex nonlinear models.

Another area for future work is to relate a suite of validation experiments and the anticipated application to our validation metrics. Just as the application can be used to help define a metric for the validation experiments, we should be able to extend this idea to multiple sets of validation experiments, each designed to test a distinct subset of the physics. This relationship should tell us how to weigh the results from the different sets of data, and whether the different sets of data adequately test the model over the anticipated range of model parameters. This context is an important link of this work to the planning approach to validation favored by the ASCI program at Sandia (Pilch, *et al.*, 2000).

Finally, we should consider using these metrics for model validation experiment design. The ideal experiment is one that minimizes our probability of rejecting a good model while maximizing our ability to reject a bad model. To do this, we will need alternative models (i.e., one good one, one bad one – but possibly not clear which is which), so that we can design the experiments to resolve the differences. The statistical metrics used to test these models should also be used to design the experiments, so that we can maximize our ability to resolve the validity of the models.

(Page left blank)

## References

- Beck, J. V. and K. J. Arnold (1977), Parameter Estimation in Engineering and Science, John Wiley & Sons, Inc., New York.
- Bell, R. L., M. R. Baer, R. M. Brannon, M. G. Elrick, E. S. Hertel, Jr., S. A. Silling, and P. A. Taylor (1998), "CTH User's Manual and Input Instructions, Version 4.0," Sandia National Laboratories, Albuquerque.
- Blackwell, B. F., R. J. Cochran, K. J. Dowding (1998), "Development and Implementation of Sensitivity Coefficient Equations for Heat Conduction Problems," Proceedings of the 7<sup>th</sup> AIAA/ASME Joint Thermophysics and Heat Transfer Conference, Albuquerque, NM, ASME HTD-Vol. 357-2, pp. 303-316.
- Brownlee, K. A. (1965), Statistical Theory and Methodology in Science and Engineering, John Wiley & Sons, Inc., New York.
- Davison, L. and R. A. Graham (1979), "Shock Compression of Solids," Phys. Reports, Vol. 55, No. 4, pp. 255-379.
- Dowding, K. J. (2000), personal communication, Sandia National Laboratories, Albuquerque.
- Dubois, D. and H. Prade (1988), Possibility Theory: An Approach to Computerized Processing of Uncertainty, Plenum, New York.
- Graham, R. A. (1993), Solids Under High-Pressure Shock Compression, Springer-Verlag, New York.
- Hertel, E. S. Jr., and G. I. Kerley (1998), "CTH EOS Package: Introductory Tutorial," Sandia National Laboratories, SAND98-0945.
- Hills, R. G. and T. G. Trucano (1999), "Statistical Validation of Engineering and Scientific Models: Background," Sandia National Laboratories, SAND99-1256.
- Hills, R. G. and T. G. Trucano (2001), "Statistical Validation of Engineering and Scientific Models with Application to CTH," Sandia National Laboratories, SAND2001-0312.
- IMSL (1997), IMSL, Math Library, Vols. 1 and 2, Visual Numerics, Inc., Houston.

- Kerley, G. I. (1998), "Theoretical Equation of State for Aluminum," *Int. J. Impact Engng.*, Vol. 5, No. 5, 441-449.
- Luis, S. J., and D. McLaughlin (1992), "A Stochastic Approach to Model Validation," *Advances in Water Resources*, Vol. 15, pp. 15-32.
- Marsh, S. P., ed. (1980), LASL Shock Hugoniot Data, University of California Press, Berkley.
- McGlaun, J. M., S. L. Thompson, and M. G. Elrick (1990), "CTH: A Three-Dimensional Shock Wave Physics Code," *Int. J. Impact Engng.*, Vol. 10, No. 1-4, pp. 351-360.
- McQueen, R. G., S. P. Marsh, J. W. Taylor, J. N. Fritz, and W. J. Carter (1970), "The Equation of State of Solids From Shock Wave Studies," in High-Velocity Impact Phenomena, ed. R. Kinslow, Academic Press, New York.
- Miller, I. and J. E. Freund (1985), Probability and Statistics for Engineers, Prentice-Hall, Inc., Englewood Cliffs, New Jersey.
- Moen, C. (1999), "FCV Users Manual," Sandia National Laboratories report, to be published.
- Pilch, M., T. Trucano, J. Moya, G. Froehlich, A. Hodges, and D. Peercy (2000), "Guidelines for Sandia ASCI Verification and Validation Plans – Content and Format: Version 2.0," Sandia National Laboratories, SAND2000-3101.
- Rice, M. H., R. G. McQueen, and J.M. Walsh (1958), "Compression of Solids by Strong Shock Waves," Solid State Physics, Vol. 6, pp. 1-63, Academic Press, New York,.
- Voth, T. E. and W. Gill (1999), "Assessment of Sub-Grid Contact Resistance Physics Effects on Thermal Simulation," Sandia National Laboratories report, to be published.
- Woolfram, S. (1999), The Mathematica Book, Cambridge University Press, New York.
- Zel'Dovich, Ya. B. and Yu. P. Raizer (1967), Physics of Shock Waves and High-Temperature Hydrodynamic Phenomena, Academic Press, New York.

## **Distribution**

### EXTERNAL DISTRIBUTION

M. A. Adams  
Jet Propulsion Laboratory  
4800 Oak Grove Drive, MS 97  
Pasadena, CA 91109

M. Aivazis  
Center for Advanced Computing  
Research  
California Institute of Technology  
1200 E. California Blvd./MS 158-79  
Pasadena, CA 91125

Charles E. Anderson  
Southwest Research Institute  
P. O. Drawer 28510  
San Antonio, TX 78284

Bilal Ayyub (2)  
Department of Civil Engineering  
University of Maryland  
College Park, MD 20742

Osman Balci  
Department of Computer Science  
Virginia Tech  
Blacksburg, VA 24061

Steven Batill (2)  
Dept. of Aerospace & Mechanical Engr.  
University of Notre Dame  
Notre Dame, IN 46556

S. Beissel  
Alliant Techsystems, Inc.  
600 Second St., NE  
Hopkins, MN 55343

David Belk  
WL/MNAA  
101 W. Eglin Blvd., Suite 219  
Eglin AFB, FL 32542-6810

Ted Belytschko (2)  
Department of Mechanical Engineering  
Northwestern University  
2145 Sheridan Road  
Evanston, IL 60208

James Berger  
Institute of Statistics and Decision Science  
Duke University  
Box 90251  
Durham, NC 27708-0251

Pavel A. Bouzinov  
ADINA R&D, Inc.  
71 Elton Avenue  
Watertown, MA 02472

John A. Cafeo  
General Motors R&D Center  
Mail Code 480-106-256  
30500 Mound Road  
Box 9055  
Warren, MI 48090-9055

James C. Cavendish  
General Motors R&D Center  
Mail Code 480-106-359  
30500 Mound Road  
Box 9055  
Warren, MI 48090-9055

Chun-Hung Chen (2)  
Associate Professor  
Department of Systems Engineering &  
Operations Research  
George Mason University  
4400 University Drive, MS 4A6  
Fairfax, VA 22030

Wei Chen  
Dept. of Mechanical Engr. (M/C 251)  
842 W. Taylor St.  
University of Illinois at Chicago  
Chicago, IL 60607-7022

Kyeongjae Cho (2)  
Dept. of Mechanical Engineering  
MC 4040  
Stanford University  
Stanford, CA 94305-4040

Thomas Chwastyk  
U.S. Navel Research Lab.  
Code 6304  
4555 Overlook Ave., SW  
Washington, DC 20375-5343

Hugh Coleman (2)  
Department of Mechanical &  
Aero. Engineering  
University of Alabama/Huntsville  
Huntsville, AL 35899

Raymond Cosner (2)  
Boeing-Phantom Works  
MC S106-7126  
P. O. Box 516  
St. Louis, MO 63166-0516

Thomas A. Cruse  
398 Shadow Place  
Pagosa Springs, CO 81147-7610

P. Cuniff  
U.S. Army Soldier Systems Center  
Kansas Street  
Natick, MA 01750-5019

Frank Dean (2)  
Strategic Systems Programs  
Nebraska Avenue Complex  
287 Somers Court NW, Suite 10041  
Washington, DC 20393-5446

Department of Energy (4)  
Attn: Kevin Greenough, DP-153  
Paul Messina, DP-51  
Juan Meza, DP-51  
William Reed, DP-51

Department of Energy  
1000 Independence Ave., SW  
Washington, DC 20585

U. M. Diwekar (2)  
Center for Energy and  
Environmental Studies  
Carnegie Mellon University  
Pittsburgh, PA 15213-3890

David Dolling  
Department of Aerospace Engineering  
& Engineering Mechanics  
University of Texas at Austin  
Austin, TX 78712-1085

Robert G. Easterling  
Department of Statistics  
4062 Frieze Bldg.  
105 S. State Street  
Ann Arbor, MI 48109-1285

Isaac Elishakoff (2)  
Dept. of Mechanical Engineering  
Florida Atlantic University  
777 Glades Road  
Boca Raton, FL 33431-0991

Joseph E. Flaherty (2)  
Dept. of Computer Science  
Rensselaer Polytechnic Institute  
Troy, NY 12181

John Fortna  
ANSYS, Inc.  
275 Technology Drive  
Canonsburg, PA 15317

Roger Ghanem  
Dept. of Civil Engineering  
Johns Hopkins University  
Baltimore, MD 21218

Mike Giltrud  
Defense Threat Reduction Agency  
DTRA/CPWS  
6801 Telegraph Road  
Alexandria, VA 22310-3398

James Glimm (2)  
Dept. of Applied Math & Statistics  
P138A  
State University of New York  
Stony Brook, NY 11794-3600

James Gran  
SRI International  
Poulter Laboratory AH253  
333 Ravenswood Avenue  
Menlo Park, CA 94025

Bernard Grossman (2)  
Dept. of Aerospace &  
Ocean Engineering  
Mail Stop 0203  
215 Randolph Hall  
Blacksburg, VA 24061

Sami Habchi  
CFD Research Corp.  
Cummings Research Park  
215 Wynn Drive  
Huntsville, AL 35805

Raphael Haftka (2)  
Dept. of Aerospace and Mechanical  
Engineering and Engineering Science  
P. O. Box 116250  
University of Florida  
Gainesville, FL 32611-6250

Achintya Haldar (2)  
Dept. of Civil Engineering  
& Engineering Mechanics  
University of Arizona  
Tucson, AZ 85721

Tim Hasselman  
ACTA  
2790 Skypark Dr., Suite 310  
Torrance, CA 90505-5345

George Hazelrigg  
Division of Design, Manufacturing  
& Innovation  
Room 508N  
4201 Wilson Blvd.  
Arlington, VA 22230

David Higdon  
Institute of Statistics and Decision Science  
Duke University  
Box 90251  
Durham, NC 27708-0251

Richard Hills (30)  
College of Engineering, MSC 3449  
New Mexico State University  
P. O. Box 30001  
Las Cruces, NM 88003

F. Owen Hoffman (2)  
SENES  
102 Donner Drive  
Oak Ridge, TN 37830

G. Ivy  
Logicon R&D Associates  
P.O. Box 92500  
Los Angeles, CA 90009

Ralph Jones (2)  
Sverdrup Tech. Inc./AEDC Group  
1099 Avenue C  
Arnold AFB, TN 37389-9013

Leo Kadanoff  
Research Institutes Building  
University of Chicago  
5640 South Ellis Ave.  
Chicago, IL 60637

George Karniadakis (2)  
Division of Applied Mathematics  
Brown University  
192 George St., Box F  
Providence, RI 02912

Alan Karr  
Institute of Statistics and Decision Science  
Duke University  
Box 90251  
Durham, NC 27708-0251

J. Keremes  
The Boeing Company  
Rocketdyne Propulsion & Power  
P. O. Box 7922  
6633 Canoga Avenue  
Canoga Park, CA 91309-7922

Hyoung-Man Kim  
Boeing Company  
M/S: ZC-01  
502 Gemini Ave.  
Houston, TX 77058

K. D. Kimsey  
U.S. Army Research Laboratory  
Weapons & Materials Research  
Directorate  
AMSRL-WM-TC 309 120A  
Aberdeen Proving Gd, MD 21005-5066

B. A. Kovac  
The Boeing Company  
Rocketdyne Propulsion & Power  
P. O. Box 7922  
6633 Canoga Avenue  
Canoga Park, CA 91309-7922

P. Krysl  
Department of Computer Science  
California Institute of Technology  
1200 E. California Blvd./MS 256-80  
Pasadena, CA 91125

W. K. Liu (2)  
Northwestern University  
Dept. of Mechanical Engineering  
2145 Sheridan Road  
Evanston, IL 60108-3111

Robert Lust  
General Motors, R&D and Planning  
MC 480-106-256  
30500 Mound Road  
Warren, MI 48090-9055

Sankaran Mahadevan (2)  
Dept. of Civil &  
Environmental Engineering  
Vanderbilt University  
Box 6077, Station B  
Nashville, TN 37235

Hans Mair  
Institute for Defense Analysis  
Operational Evaluation Division  
1801 North Beauregard Street  
Alexandria, VA 22311-1772

W. McDonald  
Naval Surface Warfare Center  
Code 420  
101 Strauss Avenue  
Indian Head, MD 20640-5035

Gregory McRae (2)  
Dept. of Chemical Engineering  
Massachusetts Institute of Technology  
Cambridge, MA 02139

Michael Mendenhall (2)  
Nielsen Engineering & Research, Inc.  
510 Clyde Ave.  
Mountain View, CA 94043

Sue Minkoff (2)  
Dept. of Mathematics and Statistics  
University of Maryland, Baltimore Co.  
1000 Hilltop Circle  
Baltimore, MD 21250

Max Morris (2)  
Department of Statistics  
Iowa State University  
304A Snedecor-Hall  
Ames, IA 50011-1210

Paul Muessig  
Naval Air Warfare Center  
Joint Accreditation Support Activity  
Weapons Division, Code 418000D  
1 Administration Circle  
China Lake, CA 93555-6100

R. Namburu  
U.S. Army Research Laboratory  
AMSRL-CI-H  
Aberdeen Proving Gd, MD 21005-5067

NASA/Ames Research Center  
Attn: U. B. Mehta  
MS: T27 B-1  
Moffett Field, CA 94035-1000

NASA/Glen Research Center  
Attn: Chris Steffen, MS 5-11  
Cleveland, OH 44135

NASA/Langley Research Center (5)  
Attn: Michael Hensch, MS 280  
Jim Luckring, MS 280  
Ahmed Noor, MS 369  
Sharon Padula, MS 159  
Hampton, VA 23681-0001

C. Needham  
Applied Research Associates, Inc.  
4300 San Mateo Blvd., Suite A-220  
Albuquerque, NM 87110

A. Needleman  
Division of Engineering, Box D  
Brown University  
Providence, RI 02912

Robert Nelson (2)  
Dept. of Aerospace &  
Mechanical Engineering  
University of Notre Dame  
Notre Dame, IN 46556

Efstratios Nikolaidis (2)  
MIME Dept.  
4035 Nitschke Hall  
University of Toledo  
Toledo, OH 43606-3390

Tinsley Oden (2)  
Texas Institute of Comp. Mechanics  
University of Texas at Austin  
Austin, TX 78712

Michael Ortiz (2)  
Graduate Aeronautical Laboratories  
California Institute of Technology  
1200 E. California Blvd./MS 105-50  
Pasadena, CA 91125

Dale Pace  
Applied Physics Laboratory  
Johns Hopkins University  
111000 Johns Hopkins Road  
Laurel, MD 20723-6099

Alex Pang  
Computer Science Department  
University of California  
Santa Cruz, CA 95064

Allan Pifko  
2 George Court  
Melville, NY 11747

Cary Presser (2)  
Process Measurements Div.  
National Institute of Standards  
and Technology  
Bldg. 221, Room B312  
Gaithersburg, MD 20899

P. Radovitzky  
Graduate Aeronautical Laboratories  
California Institute of Technology  
1200 E. California Blvd./MS 105-50  
Pasadena, CA 91125

W. Rafaniello  
DOW Chemical Company  
1776 Building  
Midland, MI 48674

Chris Rahaim (2)  
SAIC  
14 East Washington St., Suite 401  
Orlando, FL 32801-2320

Pradeep Raj (2)  
Computational Fluid Dynamics  
Lockheed Martin Aeronautical Sys.  
86 South Cobb Drive  
Marietta, GA 30063-0685

J. N. Reddy  
Dept. of Mechanical Engineering  
Texas A&M University  
ENPH Building, Room 210  
College Station, TX 77843-3123

John Renaud (2)  
Dept. of Aerospace & Mechanical Engr.  
University of Notre Dame  
Notre Dame, IN 46556

E. Repetto  
Graduate Aeronautical Laboratories  
California Institute of Technology  
1200 E. California Blvd./MS 105-50  
Pasadena, CA 91125

Patrick J. Roache  
1108 Mesa Loop NW  
Los Lunas, NM 87031

A. J. Rosakis  
Graduate Aeronautical Laboratories  
California Institute of Technology  
1200 E. California Blvd./MS 105-50  
Pasadena, CA 91125

Tim Ross (2)  
Dept. of Civil Engineering  
University of New Mexico  
Albuquerque, NM 87131

J. Sacks  
Institute of Statistics and Decision Science  
Duke University  
Box 90251  
Durham, NC 27708-0251

Sunil Saigal (2)  
Carnegie Mellon University  
Department of Civil and  
Environmental Engineering  
Pittsburgh, PA 15213

Len Schwer  
Schwer Engineering & Consulting  
6122 Aaron Court  
Windsor, CA 95492

Paul Senseny  
Factory Mutual Research Corporation  
1151 Boston-Providence Turnpike  
P.O. Box 9102  
Norwood, MA 02062

E. Sevin  
Logicon RDA, Inc.  
1782 Kenton Circle  
Lyndhurst, OH 44124

Mark Shephard (2)  
Rensselaer Polytechnic Institute  
Scientific Computation Research Center  
Troy, NY 12180-3950

T. P. Shivananda  
Bldg. SB2/Rm. 1011  
TRW/Ballistic Missiles Division  
P. O. Box 1310  
San Bernardino, CA 92402-1310

Y.-C. Shu  
Graduate Aeronautical Laboratories  
California Institute of Technology  
1200 E. California Blvd./MS 105-50  
Pasadena, CA 91125

Don Simons  
Logicon  
222 W. Sixth St.  
P.O. Box 471  
San Pedro, CA 90733-0471

Munir Sindir  
Boeing Company, MC IB39  
Rocketdyne Propulsion & Power  
P. O. Box 7922  
6633 Canoga Avenue  
Canoga Park, CA 91309-7922

Ashok Singhal (2)  
CFD Research Corp.  
Cummings Research Park  
215 Wynn Drive  
Huntsville, AL 35805

R. Singleton  
Engineering Sciences Directorate  
Army Research Office  
4300 S. Miami Blvd.  
P.O. Box 1221  
Research Triangle Park, NC 27709-2211

W. E. Snowden  
DARPA  
7120 Laketree Drive  
Fairfax Station, VA 22039

Bill Spencer (2)  
Dept. of Civil Engineering  
and Geological Sciences  
University of Notre Dame  
Notre Dame, IN 46556-0767

D. E. Stevenson (2)  
Computer Science Department  
Clemson University  
442 Edwards Hall, Box 341906  
Clemson, SC 29631-1906

Tim Swafford  
Sverdrup Tech. Inc./AEDC Group  
1099 Avenue C  
Arnold AFB, TN 37389-9013

Kenneth Tatum  
Sverdrup Tech. Inc./AEDC Group  
740 Fourth Ave.  
Arnold AFB, TN 37389-6001

Ben Thacker  
Southwest Research Institute  
6220 Culebra Road  
Postal Drawer 28510  
San Antonio, TX 78228-0510

Robert W. Walters  
Aerospace and Ocean Engineering  
Virginia Tech  
215 Randolph Hall, MS 203  
Blacksburg, VA 24061-0203

Ren-Jye Yang  
Ford Research Laboratory  
MD2115-SRL  
P.O.Box 2053  
Dearborn, MI 4812

Simone Youngblood  
DOD/DMSO  
Technical Director for VV&A  
1901 N. Beauregard St., Suite 504  
Alexandria, VA 22311

M. A. Zikry  
North Carolina State University  
Mechanical & Aerospace Engineering  
2412 Broughton Hall, Box 7910  
Raleigh, NC 27695

FOREIGN DISTRIBUTION:

Yakov Ben-Haim (2)  
Department of Mechanical Engineering  
Technion-Israel Institute of Technology  
Haifa 32000  
ISRAEL

Gert de Cooman (2)  
Universiteit Gent  
Onderzoeksgroep, SYSTeMS  
Technologiepark - Zwijnaarde 9  
9052 Zwijnaarde  
BELGIUM

Graham de Vahl Davis (2)  
CFD Research Laboratory  
University of NSW  
Sydney, NSW 2052  
AUSTRALIA

Luis Eca (2)  
Instituto Superior Tecnico  
Department of Mechanical Engineering  
Av. Rovisco Pais  
1096 Lisboa CODEX  
PORTUGAL

Charles Hirsch (2)  
Department of Fluid Mechanics  
Vrije Universiteit Brussel  
Pleinlaan, 2  
B-1050 Brussels  
BELGIUM

Igor Kozin  
Systems Analysis Department  
Riso National Laboratory  
P. O. Box 49  
DK-4000 Roskilde  
DENMARK

K. Papoulia  
Inst. Eng. Seismology & Earthquake  
Engineering  
P.O. Box 53, Finikas GR-55105  
Thessaloniki  
GREECE

Malcolm Wallace  
National Engineering Laboratory  
East Kilbride  
Glasgow  
G75 0QU  
UNITED KINGDOM

Peter Walley  
36 Bloomfield Terrace  
Lower Hutt  
NEW ZEALAND

Dr. Max Ruppert  
UniBw Munich - BauV 2.2  
Inst. Engng.Mech. & Struct.Mech.  
D - 85577 Neuibiberg  
GERMANY

Los Alamos National Laboratory (40)  
Mail Station 5000  
P.O. Box 1663  
Los Alamos, NM 87545

Attn: Peter Adams, MS B220  
Attn: Mark C. Anderson, MS D411  
Attn: Thomas Bement, MS F600  
Attn: Terrence Bott, MS K557  
Attn: D. Cagliostro, MS F645  
Attn: David Crane, MS P946  
Attn: John F. Davis, MS B295  
Attn: Helen S. Deaven, MS B295  
Attn: Scott Doebbling, MS P946  
Attn: S. Eisenhower, MS K557  
Attn: Dawn Flicker, MS F664  
Attn: George T. Gray, MS G755  
Attn: Ken Hanson, MS P940  
Attn: R. Henninger, MS D413  
Attn: Brad Holian, MS B268  
Attn: Kathleen Holian, MS B295  
Attn: Darryl Holm, MS B284  
Attn: James Hyman, MS B284  
Attn: Michael E. Jones, MS B259  
Attn: Cliff Joslyn, MS B265  
Attn: James Kamm, MS D413  
Attn: Joseph Kindel, MS B259  
Attn: Jeanette Lagrange, MS D445  
Attn: S. Keller-McNulty, MS F600  
Attn: Elizabeth Kelly, MS F600  
Attn: Ken Koch, MS F652  
Attn: Len Margolin, MS D413  
Attn: Harry Martz, MS F600  
Attn: Mike McKay, MS F600  
Attn: Kelly McLenithan, MS F664  
Attn: Mark P. Miller, MS P946  
Attn: John D. Morrison, MS F602  
Attn: Karen I. Pao, MS B256  
Attn: M. Peterson-Schnell,  
MS B295  
Attn: Douglas Post, MS F661 X-DO  
Attn: William Rider, MS D413

Attn: Tom Seed, MS F663	1	MS 0482 2109	S. E. Lott
Attn: David Sharp, MS B213	1	MS 0447 2111	J. O. Harrison
Attn: Richard N. Silver, MS D429	1	MS 0447 2111	P. D. Hoover
Attn: Ronald E. Smith, MS J576	1	MS 0479 2151	P. A. Sena
Attn: Christine Treml, MS H851	1	MS 0479 2151	M. H. Abt
Attn: David Tubbs, MS B220	1	MS 0482 2161	V. J. Johnson
Attn: Daniel Weeks, MS B295	1	MS 0482 2161	R. S. Baty
Attn: Morgan White, MS F663	1	MS 0481 2167	M. A. Rosenthal
Attn: Alyson G. Wilson, MS F600	1	MS 0481 2167	W. C. Moffatt
	1	MS 0481 2168	K. D. Meeks
University of California (20)	1	MS 0481 2168	K. Ortiz
Lawrence Livermore National Laboratory	1	MS 0509 2300	M. W. Callahan
7000 East Ave.	1	MS 0634 2951	K. V. Chavez
P.O. Box 808	1	MS 0769 5800	D. S. Miyoshi
Livermore, CA 94550	1	MS 0759 5845	I. V. Waddoups
Attn: T. F. Adams, MS L-095	1	MS 0759 5845	M. S. Tierney
Attn: Steven Ashby, MS L-561	1	MS 0782 5861	R. V. Matalucci
Attn: John Bolstad, MS L-023	1	MS 0737 6114	P. A. Davis
Attn: Peter N. Brown, MS L-561	1	MS 0751 6117	L. S. Costin
Attn: T. Scott Carman, MS L-031	1	MS 0718 6141	C. D. Massey
Attn: R. Christensen, MS L-160	1	MS 0708 6214	P. S. Veers
Attn: Evi Dube, MS L-095	1	MS 0747 6410	R. L. Camp
Attn: Richard Klein, MS L-023	1	MS 0747 6410	G. D. Wyss
Attn: Roger Logan, MS L-125	1	MS 0746 6411	R. M. Cranwell
Attn: C. F. McMillan, MS L-098	1	MS 0746 6411	D. J. Anderson
Attn: C. Mailhiot, MS L-055	1	MS 0746 6411	J. E. Campbell
Attn: J. F. McEnerney, MS L-023	1	MS 0746 6411	D. G. Robinson
Attn: M. J. Murphy, MS L-282	1	MS 0744 6400	D. A. Powers
Attn: Daniel Nikkel, MS L-342	1	MS 0746 6411	L. P. Swiler
Attn: Cynthia Nitta, MS L-096	1	MS 0748 6413	R. D. Waters
Attn: Peter Raboin, MS L-125	1	MS 1140 6500	J. K. Rice
Attn: Peter Terrill, MS L-125	1	MS 0974 6522	G. D. Valcez
Attn: Charles Tong, MS L-560	1	MS 0977 6524	W. R. Cook
	3	MS 0977 6524	S. M. DeLand
Argonne National Laboratory	1	MS 1138 6533	E. Shepherd
Attn: Paul Hovland	1	MS 1138 6534	L. M. Claussen
MCS Division	1	MS 1137 6534	A. L. Hodges
Bldg. 221, Rm. C-236	1	MS 1138 6534	M. T. McCornack
9700 S. Cass Ave.	1	MS 1137 6534	S. V. Romero
Argonne, IL 60439	1	MS 1137 6535	G. K. Froehlich
	1	MS 0771 6805	P. G. Kaplan
SANDIA INTERNAL	1	MS 1395 6821	J. W. Garner
	1	MS 1395 6821	P. Vaughn
1 MS 1152 1642 M. L. Kiefer	1	MS 0779 6849	J. C. Helton
1 MS 1186 1674 R. J. Lawrence	1	MS 0779 6849	R. P. Rechar
1 MS 0525 1734 P. V. Plunkett	1	MS 0779 6849	M. J. Shortencarier
1 MS 0525 1734 R. B. Heath	1	MS 0778 6851	G. E. Barr
1 MS 0525 1734 S. D. Wix	1	MS 0778 6851	R. J. MacKinnon
1 MS 1393 1902 J. R. Garcia	1	MS 9051 8351	C. A. Kennedy
1 MS 0457 2001 W. J. Tedeschi	1	MS 9202 8418	W. P. Ballard
1 MS 0429 2100 J. S. Rottler	1	MS 9202 8418	R. M. Zurn
1 MS 0453 2104 D. L. McCoy	1	MS 9405 8700	T. M. Dyer
1 MS 0475 2105 R. C. Hartwig	1	MS 9042 8725	W. A. Kawahara
1 MS 1393 2106 F. F. Dean	1	MS 9405 8726	R. E. Jones
1 MS 0482 2109 R. A. Paulsen	1	MS 9161 8726	P. A. Klein

1	MS 9161 8726	E. P. Chen	1	MS 0557 9125	T. J. Baca
1	MS 9042 8728	C. D. Moen	1	MS 0557 9125	C. C. O’Gorman
1	MS 9405 8743	R. A. Regueiro	1	MS 0553 9126	R. A. May
1	MS 9003 8900	K. E. Washington	1	MS 0847 9126	S. N. Burchett
1	MS 9012 8920	P. E. Nielan	1	MS 0847 9126	K. E. Metzinger
1	MS 9217 8950	P. T. Boggs	1	MS 0824 9130	J. L. Moya
1	MS 9217 8950	P. D. Hough	1	MS 0821 9132	L. A. Gritzo
1	MS 9217 8950	M. L. Martinez-Canales	3	MS 0828 9133	M. Pilch
1	MS 9217 8950	M. L. Koszykowski	1	MS 0828 9133	A. R. Black
1	MS 1110 8950	L. J. Lehoucq	1	MS 0828 9133	B. F. Blackwell
1	MS 9217 8950	K. R. Long	1	MS 0828 9133	K. J. Dowding
1	MS 0841 9100	T. C. Bickel	1	MS 0828 9133	W. L. Oberkampf
1	MS 0836 9100	M. R. Baer	1	MS 0557 9133	T. L. Paez
1	MS 0824 9100	T. Y. Chu	1	MS 0828 9133	V. J. Romero
1	MS 0841 9100	C. W. Peterson	1	MS 0557 9133	A. Urbina
1	MS 0835 9100	D. K. Gartling	1	MS 0847 9133	W. R. Witkowski
1	MS 0834 9112	A. C. Ratzel	1	MS 1135 9134	S. Heffelfinger
1	MS 0826 9113	W. Hermina	1	MS 0555 9134	J. T. Nakos
1	MS 0826 9113	T. J. Bartel	1	MS 0835 9140	J. M. McGlaun
1	MS 0827 9114	J. E. Johannes	1	MS 0835 9140	J. A. Fernandez
1	MS 0827 9114	K. S. Chen	1	MS 0835 9140	A. Gurule
1	MS 0827 9114	L. A. Mondy	1	MS 0835 9140	R. Garber
1	MS 0827 9114	R. R. Rao	1	MS 0835 9141	S. N. Kempka
1	MS 0827 9114	P. R. Schunk	1	MS 0835 9141	S. P. Burns
3	MS 0825 9115	W. H. Rutledge	1	MS 0835 9141	R. J. Cochran
3	MS 0825 9115	S. J. Beresh	1	MS 0835 9141	B. Hassan
3	MS 0825 9115	F. G. Blottner	1	MS 0835 9141	C. Roy
3	MS 0825 9115	D. W. Kuntz	1	MS 0835 9142	J. S. Peery
1	MS 0825 9115	M. A. McWherter Payne	1	MS 0847 9142	S. W. Attaway
3	MS 0825 9115	J. L. Payne	1	MS 0847 9142	M. L. Blanford
3	MS 0825 9115	D. L. Potter	1	MS 0847 9142	M. W. Heinstein
1	MS 0825 9115	K. Salari	1	MS 0847 9142	S. W. Key
1	MS 0825 9115	L. W. Young	1	MS 0847 9142	G. M. Reese
1	MS 0825 9115	W. P. Wolfe	1	MS 0835 9142	J. R. Weatherby
1	MS 0836 9116	E. S. Hertel	1	MS 0826 9143	J. D. Zepper
1	MS 0836 9116	C. Romero	1	MS 0827 9143	K. M. Aragon
1	MS 0836 9116	S. R. Tieszen	1	MS 0827 9143	H. C. Edwards
1	MS 0827 9117	R. O. Griffith	1	MS 0847 9143	G. D. Sjaardema
1	MS 0367 9117	R. J. Buss	1	MS 0826 9143	J. R. Stewart
1	MS 0827 9117	R. B. Campbell	1	MS 0321 9200	W. J. Camp
1	MS 0827 9117	D. Dobranich	1	MS 0318 9200	G. S. Davidson
1	MS 0836 9117	R. E. Hogan	1	MS 0310 9209	G. S. Heffelfinger
1	MS 0827 9117	T. E. Voth	1	MS 1111 9209	S. J. Plimpton
1	MS 0847 9120	H. S. Morgan	1	MS 1110 9211	D. E. Womble
1	MS 0555 9122	M. S. Garrett	1	MS 1110 9211	R. Carr
1	MS 0847 9123	A. F. Fossum	1	MS 1110 9211	S. Y. Chakerian
1	MS 0847 9124	D. R. Martinez	1	MS 0847 9211	M. S. Eldred
3	MS 0847 9124	K. F. Alvin	1	MS 0847 9211	A. A. Giunta
1	MS 0847 9124	T. B. Carne	1	MS 1110 9211	W. E. Hart
1	MS 0847 9124	J. L. Dohner	1	MS 1110 9211	A. Johnson
1	MS 0847 9124	R. V. Field	1	MS 1110 9211	V. J. Leung
1	MS 0847 9124	T. Simmermacher	1	MS 1110 9211	C. A. Phillips
1	MS 0847 9124	D. O. Smallwood	1	MS 0847 9211	J. R. Red-Horse
1	MS 0847 9124	S. F. Wojtkiewicz, Jr.	20	MS 0819 9211	T. G. Trucano

1	MS 0847 9211	B. A. vanBloemen Waanders	1	MS 0434 12334	R. J. Breeding
1	MS 1109 9212	R. J. Pryor	3	MS 0829 12335	K. V. Diegert
1	MS 1110 9214	J. DeLaurentis	1	MS 1221 15002	R. D. Skocypec
1	MS 1110 9214	R. B. Lehoucq	1	MS 1179 15340	J. R. Lee
1	MS 0321 9220	A. L. Hale	1	MS 1179 15341	L. J. Lorence
1	MS 1110 9223	N. D. Pundit	1	MS 0301 15400	J. L. McDowell
1	MS 0321 9224	J. A. Ang	1	MS 9018 8945-1	Central Technical Files
1	MS 0321 9224	R. E. Benner	2	MS 0899 9616	Technical Library
1	MS 0321 9224	J. L. Tompkins	1	MS 0612 9612	Review & Approval Desk For DOE/OSTI
1	MS 0847 9226	R. W. Leland			
1	MS 0847 9226	B. A. Hendrickson			
1	MS 0847 9226	P. Knupp			
1	MS 0318 9227	P. D. Heermann			
1	MS 0318 9227	C. F. Diegert			
1	MS 0310 9230	P. Yarrington			
1	MS 0819 9231	E. A. Boucheron			
1	MS 0819 9231	K. H. Brown			
1	MS 0819 9231	K. G. Budge			
1	MS 0819 9231	D. E. Carroll			
1	MS 0819 9231	M. Christon			
1	MS 0819 9231	R. R. Drake			
1	MS 0819 9231	A. C. Robinson			
1	MS 0819 9231	R. M. Summers			
1	MS 0819 9231	M. K. Wong			
1	MS 0820 9232	P. F. Chavez			
1	MS 0820 9232	R. M. Brannon			
1	MS 0820 9232	M. E. Kipp			
1	MS 0820 9232	S. A. Silling			
1	MS 0820 9232	P. A. Taylor			
1	MS 0316 9233	S. S. Dosanjh			
1	MS 1111 9233	D. Gardner			
1	MS 1111 9233	A. G. Salinger			
1	MS 1111 9233	J. N. Shadid			
1	MS 0316 9235	J. B. Aidun			
1	MS 1111 9235	H. P. Hjalmarson			
1	MS 0660 9519	D. S. Eaton			
1	MS 0660 9519	M. A. Ellis			
1	MS 0421 9814	J. M. Sjulín			
1	MS 0423 9817	R. A. Paulsen			
1	MS 0423 9817	S. E. Dingman			
1	MS 0139 9900	M. O. Vahle			
1	MS 0139 9904	R. K. Thomas			
1	MS 0428 12300	D. D. Carlson			
1	MS 0490 12331	J. A. Cooper			
1	MS 0829 12323	F. W. Spencer			
1	MS 0829 12323	M. L. Abate			
1	MS 0829 12323	R. G. Easterling			
3	MS 0829 12323	B. M. Rutherford			
1	MS 0638 12326	M. A. Blackledge			
1	MS 0638 12326	D. E. Peercy			
1	MS 0638 12326	D. L. Knirk			
1	MS 0490 12331	P. E. D'Antonio			
1	MS 0492 12332	D. R. Olson			
1	MS 0405 12333	T. R. Jones			